**Nationaal Lucht- en Ruimtevaartlaboratorium**
National Aerospace Laboratory NLR

NLR TP 96297 U

# Adaptive grid generation by using the Laplace-Beltrami operator on a monitor surface

S.P. Spekreijse, R. Hagmeijer, J.W. Boerstoel

DOCUMENT CONTROL SHEET

| | ORIGINATOR'S REF.<br>NLR TP 96297 U | | SECURITY CLASS.<br>Unclassified |
|---|---|---|---|

ORIGINATOR
National Aerospace Laboratory NLR, Amsterdam, The Netherlands

TITLE
Adaptive grid generation by using the Laplace-Beltrami operator on a monitor surface

PRESENTED AT
5th International Conference on Numerical Grid Generation in Computational Field Simulations, Mississippi State University, USA,
April 1 - April 5, 1996

| AUTHORS | DATE | pp | ref |
|---|---|---|---|
| S.P. Spekreijse, R. Hagmeijer, J.W. Boerstoel | 960501 | 43 | 8 |

DESCRIPTORS

| | |
|---|---|
| Adaption | Harmonic functions |
| Algorithms | Laplace-Beltrami equation |
| Boundary conditions | Navier-Stokes equation |
| Dirichlet problem | Orthogonality |
| Grid generation (mathematics) | Shock wave interaction |

ABSTRACT
A two-dimensional solution-adaptive grid generation method based on mesh movement is presented. As explained in Ref. 1, each simply connected domain *D* in 2D physical space which is bounded by four edge-curves, can be mapped one-to-one onto a square parameter space Pst. This harmonic map only depends on the shape of the domain. Using this map, an initial grid in domain D can be mapped into the parameter space and yields a corresponding initial grid in that space. In parameter space, the solution vector is considered as a monitor surface and the Laplace-Beltrami equation is used to cover the monitor surface with a uniform distribution of grid points. The projection of these points on the (s, t) plane define the adapted grid in parameter space Pst. After that, the harmonic map can then be used to map the adapted grid from parameter space into the physical space.

## Summary

A two-dimensional solution-adaptive grid generation method based on mesh movement is presented. As explained in Ref. 1, each simply connected domain $\mathcal{D}$ in 2D physical space which is bounded by four edge-curves, can be mapped one-to-one onto a square parameter space $\mathcal{P}_{st}$. This harmonic map only depends on the shape of the domain. Using this map, an initial grid in domain $\mathcal{D}$ can be mapped into the parameter space and yields a corresponding initial grid in that space. In parameter space, the solution vector is considered as a monitor surface and the Laplace-Beltrami equation is used to cover the monitor surface with a uniform distribution of grid points. The projection of these points on the $(s, t)$ plane define the adapted grid in parameter space $\mathcal{P}_{st}$. After that, the harmonic map can then be used to map the adapted grid from parameter space into the physical space.

## Contents

**1 Introduction** 5

**2 The Laplace-Beltrami operator** 6

**3 Grid adaptation in parameter space $\mathcal{P}_{st}$** 9

**4 Numerical aspects** 13

**5 Illustrations** 15

**6 Conclusions** 17

**7 References** 18

(43 pages in total)

## 1 Introduction

The theory of harmonic maps is becoming increasingly popular for the construction of adaptive grids. The popularity of the use of harmonic maps for grid adaptation comes from the fact that the adaptive meshes are continuous and differentiable with non-vanishing Jacobian. This very important property guarantees one-to-one mapping.

In Refs. 6, 7, the grid was adapted in a domain in physical space by prescribing a special metric in it. Even more closely related to this investigation is the work of Ivanenko (Ref. 8), who obtained adaptive grids by projecting harmonic coordinates constructed on the surface of graph of the monitor surface on the given domain in physical space. A variational approach has been used, based on the approximation of the harmonic functional (Dirichlet's functional) itself rather then the Euler equations.

In this paper, the problem of grid adaptation in a domain in physical space is broken into two subproblems. First the grid adaptation is formulated in parameter space (a simple unit square), by using the harmonic map between the domain in physical space and the parameter space (see Ref. 1). The harmonic map only depends on the shape of the domain and can therefore be considered as a property of the domain. The harmonic map is used to map the initial grid from the physical domain into the parameter space. In parameter space, the solution vector is considered as a monitor surface (see Ref. 2). The solution of the Laplace-Beltrami equation yields an harmonic map from the graph of the monitor surface onto the computational space (a unit square supplied with a uniform mesh). The inverse mapping from computational space to the monitor surface defines harmonic coordinates on the surface which are then projected onto the $(s, t)$ plane. The projection of these points define the adapted grid in parameter space $\mathcal{P}_{st}$. The inverse map is easily obtained by numerical inversion instead of interchanging dependent and independent variables which is the more common approach. Finally the harmonic map between the parameter space and the physical domain can be used to map the adapted grid from parameter space into the physical space.

## 2 The Laplace-Beltrami operator

Consider a bounded surface $\mathcal{S}$ with a prescribed geometrical shape in three dimensional physical space with Cartesian coordinates $\vec{x} = (x, y, z)^T$. Assume that $\mathcal{S}$ is parametrized by a differentiable one-to-one mapping $\vec{x} : \mathcal{P}_{st} \mapsto \mathcal{S}$, where $\mathcal{P}_{st}$ is the unit square in two dimensional space with Cartesian coordinates $\vec{s} = (s, t)^T$. Let $(E_1, E_2)$ and $(E_3, E_4)$ be the two pairs of opposite edges of surface $\mathcal{S}$. Assume that $s \equiv 0$ at edge $E_1$, $s \equiv 1$ at edge $E_2$, $t \equiv 0$ at edge $E_3$, $t \equiv 1$ at edge $E_4$. Introduce the two covariant base vectors

$$\vec{a}_1 = \frac{\partial \vec{x}}{\partial s} = \vec{x}_s \ , \ \vec{a}_2 = \frac{\partial \vec{x}}{\partial t} = \vec{x}_t. \tag{1}$$

The two covariant base vectors span the tangent plane of $\mathcal{S}$ at the corresponding point $P$. The two contravariant base vectors $\vec{a}^1$ and $\vec{a}^2$ are also lying in the tangent plane of $\mathcal{S}$ at the corresponding point $P$, and obey

$$(\vec{a}^i, \vec{a}_j) = \delta^i_j \ \ i = \{1, 2\} \ , \ j = \{1, 2\}, \tag{2}$$

where $\delta^i_j$ is the Kronecker symbol. Define the covariant metric tensor components $a_{ij} = (\vec{a}_i, \vec{a}_j)$, and the contravariant metric tensor components $a^{ij} = (\vec{a}^i, \vec{a}^j)$. The covariant and contravariant metric tensor components are related to each other according to

$$\begin{pmatrix} a_{11} & a_{12} \\ a_{12} & a_{22} \end{pmatrix} \begin{pmatrix} a^{11} & a^{12} \\ a^{12} & a^{22} \end{pmatrix} = \begin{pmatrix} 1 & 0 \\ 0 & 1 \end{pmatrix}. \tag{3}$$

Furthermore, $\vec{a}^1 = a^{11}\vec{a}_1 + a^{12}\vec{a}_2$ and $\vec{a}^2 = a^{12}\vec{a}_1 + a^{22}\vec{a}_2$. Introduce the determinant $J^2$ of the covariant metric tensor: $J^2 = a_{11}a_{22} - a^2_{12}$. Note that $J$ is equal to the area spanned by the vectors $\vec{a}_1$ and $\vec{a}_2$ i.e. $J = \| \vec{a}_1 \wedge \vec{a}_2 \|$, where $\wedge$ is the vector product operator.

Now consider an arbitrary function $\phi = \phi(s, t)$. Then $\phi$ is also defined on surface $\mathcal{S}$ and the gradient of $\phi$ is equal to

$$\nabla\phi = \text{ grad } \phi = \phi_s\vec{a}^1 + \phi_t\vec{a}^2 \tag{4}$$

and the Laplace-Beltrami operator $\triangle\phi$ is equal to

$$\triangle\phi = \text{div ( grad } \phi) = \frac{1}{J}\left\{\left(Ja^{11}\phi_s + Ja^{12}\phi_t\right)_s + \left(Ja^{12}\phi_s + Ja^{22}\phi_t\right)_t\right\}, \tag{5}$$

which may be found in every textbook on Tensor Analysis and Differential Geometry (for example see Ref. 4, section 77, page 225). According to the RHS of Eq.(5), the Laplace-Beltrami equation $\triangle\phi = 0$ can be written in vector notation as

$$\text{div } (M \text{ grad } \phi) = 0 \tag{6}$$

where the matrix $M = M(s,t)$ is defined as

$$M = J\begin{pmatrix} a^{11} & a^{12} \\ a^{12} & a^{22} \end{pmatrix} = \frac{1}{J}\begin{pmatrix} a_{22} & -a_{12} \\ -a_{12} & a_{11} \end{pmatrix}. \tag{7}$$

In Eq.(6), the div and grad operator are now operators in parameter space $\mathcal{P}_{st}$.

Consider the generalized Dirichlet integral

$$I(\phi) = \int\int_{\mathcal{P}_{st}} (\nabla\phi, \nabla\phi) J ds dt = \int\int_{\mathcal{P}_{st}} (a^{11}\phi_s^2 + 2a^{12}\phi_s\phi_t + a^{22}\phi_t^2) J ds dt. \tag{8}$$

The associated Euler equation for the minimization of $I$ is given by

$$\left(Ja^{11}\phi_s + Ja^{12}\phi_t\right)_s + \left(Ja^{12}\phi_s + Ja^{22}\phi_t\right)_t = 0. \tag{9}$$

Thus the Laplace-Beltrami equation is the Euler equation of the generalized Dirichlet integral.

Introduce the parameter space $\mathcal{P}_{\xi\eta}$ as the unit square in a two dimensional space with Cartesian coordinates $\vec{\xi} = (\xi, \eta)^T$. Require that the parameters $\xi$ and $\eta$ obey the following boundary conditions: • $\xi \equiv 0$ at edge $E_1$ and $\xi \equiv 1$ at edge $E_2$, • $\xi$ obeys natural boundary conditions at edges $E_3$ and $E_4$, • $\eta \equiv 0$ at edge $E_3$ and $\eta \equiv 1$ at edge $E_4$, • $\eta$ obeys natural boundary conditions at

edges $E_1$ and $E_2$. Furthermore, require that

$$\text{div } (M \text{ grad } \xi) = 0 \, , \text{ div } (M \text{ grad } \eta) = 0. \tag{10}$$

The natural boundary condition for $\eta = \eta(s,t)$ along edge $E_1$ $(E_2)$, is obtained as follows. Consider a curve $\eta(s,t) = \eta_0 = constant$ in parameter space $\mathcal{P}_{st}$. Assume that this curve can be parametrized, i.e. $s = s(\alpha)$, $t = t(\alpha)$, so that $\eta(s(\alpha), t(\alpha)) = \eta_0$. Differentiation w.r.t. $\alpha$ gives $\eta_s s_\alpha + \eta_t t_\alpha = 0$. The corresponding curve on surface $\mathcal{S}$ is defined as $\vec{x}(\alpha) = \vec{x}(s(\alpha), t(\alpha))$. Hence $\vec{x}_\alpha = \vec{x}_s s_\alpha + \vec{x}_t t_\alpha$. The natural boundary condition along edge $E_1$ $(E_2)$ requires that the curve $\vec{x}(\alpha) = \vec{x}(s(\alpha), t(\alpha))$ is orthogonal at edge $E_1$ $(E_2)$ on surface $\mathcal{S}$. Thus $(\vec{x}_\alpha, \vec{x}_t) = 0$. This yields $(\vec{x}_s, \vec{x}_t) s_\alpha + (\vec{x}_t, \vec{x}_t) t_\alpha = 0$. Using this relation, together with $\eta_s s_\alpha + \eta_t t_\alpha = 0$, yields the natural boundary condition for $\eta = \eta(s,t)$ along edge $E_1$ $(E_2)$:

$$\eta_s = \frac{(\vec{x}_s, \vec{x}_t)}{(\vec{x}_t, \vec{x}_t)} \eta_t. \tag{11}$$

In the same way, the natural boundary condition for $\xi = \xi(s,t)$ along edge $E_3$ $(E_4)$ is

$$\xi_t = \frac{(\vec{x}_s, \vec{x}_t)}{(\vec{x}_s, \vec{x}_s)} \xi_s. \tag{12}$$

The field equations div $(M$ grad $\xi) = 0$ and div $(M$ grad $\eta) = 0$, supplied with the boundary conditions, define the mapping $\vec{\xi} : \mathcal{P}_{st} \mapsto \mathcal{P}_{\xi\eta}$. Now, suppose that the parameter space $\mathcal{P}_{\xi\eta}$ is covered by a uniform mesh. Inversion of the mapping $\vec{\xi} : \mathcal{P}_{st} \mapsto \mathcal{P}_{\xi\eta}$ yields a corresponding mesh in parameter space $\mathcal{P}_{st}$, which can be mapped onto surface $\mathcal{S}$. This mesh will cover surface $\mathcal{S}$ with a Laplace mesh, i.e. a smooth mesh with slowly varying mesh-line density. This observation will be the basis for our grid adaptation algorithm.

## 3 Grid adaptation in parameter space $\mathcal{P}_{st}$

Consider a simply connected bounded domain $\mathcal{D}$ in two dimensional space with Cartesian coordinates $\vec{x} = (x, y)^T$. Let $(E_1, E_2)$ and $(E_3, E_4)$ be the two pairs of opposite edges as shown in Fig.1. Suppose that domain $\mathcal{D}$ is covered by an initial grid. Let this grid be given by the mapping $\vec{x}^I : \mathcal{P}_{\xi\eta} \mapsto \mathcal{D}$ which maps a uniform grid in computational space $\mathcal{P}_{\xi\eta}$ into $\mathcal{D}$. Assume that this mapping is such that $\xi \equiv 0$ at edge $E_1$, $\xi \equiv 1$ at edge $E_2$, $\eta \equiv 0$ at edge $E_3$, $\eta \equiv 1$ at edge $E_4$.

We wish to adapt the grid to a given solution vector $\vec{Q}_{\mathcal{D}} = \vec{Q}_{\mathcal{D}}(\vec{x})$ of some initial-boundary value problem for flow equations. For this purpose, we use the same parameter space $\mathcal{P}_{st}$ as introduced in Ref. 1 for elliptic grid generation. As in Ref. 1, the parameter space $\mathcal{P}_{st}$ is defined as the unit square in a two dimensional space with Cartesian coordinates $\vec{s} = (s, t)^T$. The parameters $s$ and $t$ obey the following boundary conditions: • $s \equiv 0$ at edge $E_1$ and $s \equiv 1$ at edge $E_2$, • $s$ is the normalized arc length along edges $E_3$ and $E_4$, • $t \equiv 0$ at edge $E_3$ and $t \equiv 1$ at edge $E_4$, • $t$ is the normalized arc length along edges $E_1$ and $E_2$. The mapping $\vec{s} : \partial\mathcal{D} \mapsto \partial\mathcal{P}_{st}$ is defined by these requirements. In the interior of $\mathcal{D}$, the parameters $s$ and $t$ are harmonic functions of $x$ and $y$, thus obey the Laplace equations $\triangle s = s_{xx} + s_{yy} = 0$ and $\triangle t = t_{xx} + t_{yy} = 0$. The two Laplace equations $\triangle s = 0$ and $\triangle t = 0$, together with the above specified boundary conditions, define the harmonic mapping $\vec{s} : \mathcal{D} \mapsto \mathcal{P}_{st}$. Note that this mapping only depends on the shape of domain $\mathcal{D}$ and may thus be considered as a property of domain $\mathcal{D}$. It is well known that this mapping is differentiable and one-to-one, so that the inverse mapping also exist. The inverse mapping $\vec{x} : \mathcal{P}_{st} \mapsto \mathcal{D}$ is called the elliptic transformation.

Due to the fact that there is an initial grid in domain $\mathcal{D}$, presented by the mapping $\vec{x}^I : \mathcal{P}_{\xi\eta} \mapsto \mathcal{D}$, the corresponding grid in parameter space $\mathcal{P}_{st}$ can be easily computed by solving, in $\mathcal{D}$, the Laplace equations supplied with the Dirichlet boundary conditions. Let this grid be given by the mapping $\vec{s}^I : \mathcal{P}_{\xi\eta} \mapsto \mathcal{P}_{st}$. The idea is to adapt mapping $\vec{s}^I$, i.e. the initial grid in parameter space $\mathcal{P}_{st}$.

Grid adaptation in parameter space $\mathcal{P}_{st}$ has several useful properties (see Ref. 3). The solution vector $\vec{Q}_{\mathcal{D}}$ at a grid point of the initial grid in $\mathcal{D}$, can be transfered to the corresponding grid point of the initial grid in $\mathcal{P}_{st}$. Let $\vec{Q}_{\mathcal{P}_{st}}$ represent the solution vector in $\mathcal{P}_{st}$. One of the problems in grid adaptation is the scaling of the solution vector. The components of $\vec{Q}_{\mathcal{D}}$ may have different dimensions and represent quantities like density, velocity, pressure etc. A natural way to scale $\vec{Q}_{\mathcal{P}_{st}}$ is to normalize each component such that it is dimensionless and has range $[-1, 1]$.

Because parameter space $\mathcal{P}_{st}$ can be considered as the normalized arc length scaled space of domain

$\mathcal{D}$, the initial grid in $\mathcal{D}$ and the corresponding initial grid in $\mathcal{P}_{st}$ will share the same properties. For example, when the initial grid in $\mathcal{D}$ has a refined structure in a boundary-layer or a shock, then these refined structures will also exist in the corresponding initial grid in $\mathcal{P}_{st}$.

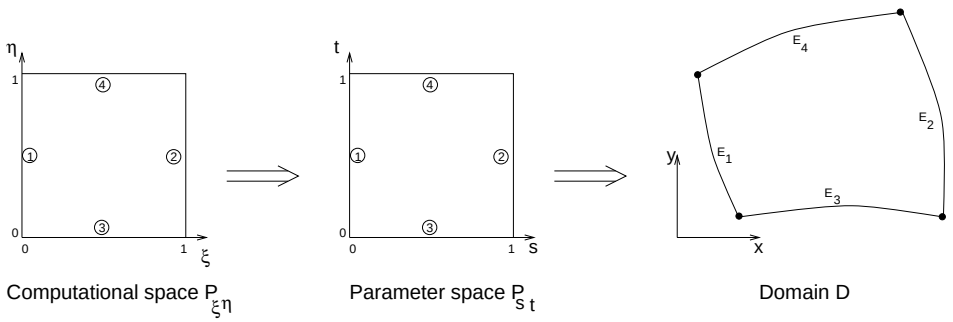


*Fig. 1 Transformation from computational space $\mathcal{P}_{\xi\eta}$, via parameter space $\mathcal{P}_{st}$, to domain $\mathcal{D}$ in Cartesian $(x, y)$ space.*

After adaptation in $\mathcal{P}_{st}$, the adapted grid in $\mathcal{P}_{st}$ must be mapped into domain $\mathcal{D}$. The elliptic grid generation method, presented in Ref. 1, can be used to generate the adapted grid in domain $\mathcal{D}$. Let the mapping $\vec{s}^A : \mathcal{P}_{\xi\eta} \mapsto \mathcal{P}_{st}$, with components $s = s^A(\xi, \eta)$ and $t = t^A(\xi, \eta)$, represent the adapted grid in $\mathcal{P}_{st}$. Then it is found in Ref. 1 that the adapted grid in $\mathcal{D}$, represented by the mapping $\vec{x}^A : \mathcal{P}_{\xi\eta} \mapsto \mathcal{D}$, obeys the Poisson system:

$$\begin{aligned} b_{22}\vec{x}^A_{\xi\xi} - 2b_{12}\vec{x}^A_{\xi\eta} + b_{11}\vec{x}^A_{\eta\eta} \quad &+ \quad \left(b_{22}P^1_{11} - 2b_{12}P^1_{12} + b_{11}P^1_{22}\right)\vec{x}^A_{\xi} \\ &+ \quad \left(b_{22}P^2_{11} - 2b_{12}P^2_{12} + b_{11}P^2_{22}\right)\vec{x}^A_{\eta} = 0, \end{aligned} \tag{13}$$

where $b_{11}, b_{12}, b_{11}$ are the covariant tensor components defined by

$$b_{11} = (\vec{x}^A_{\xi}, \vec{x}^A_{\xi}) \ , \ b_{12} = (\vec{x}^A_{\xi}, \vec{x}^A_{\eta}) \ , \ b_{22} = (\vec{x}^A_{\eta}, \vec{x}^A_{\eta}), \tag{14}$$

and where

$$\vec{P}_{11} = -T^{-1}\begin{pmatrix} s^A_{\xi\xi} \\ t^A_{\xi\xi} \end{pmatrix} \ , \ \vec{P}_{12} = -T^{-1}\begin{pmatrix} s^A_{\xi\eta} \\ t^A_{\xi\eta} \end{pmatrix} \ , \ \vec{P}_{22} = -T^{-1}\begin{pmatrix} s^A_{\eta\eta} \\ t^A_{\eta\eta} \end{pmatrix}, \tag{15}$$

with the matrix $T$ is defined as

$$T = \begin{pmatrix} s_\xi^A & s_\eta^A \\ t_\xi^A & t_\eta^A \end{pmatrix}. \tag{16}$$

The six coefficients of the vectors $\vec{P}_{11} = (P_{11}^1, P_{11}^2)^T$ , $\vec{P}_{12} = (P_{12}^1, P_{12}^2)^T$ and $\vec{P}_{22} = (P_{22}^1, P_{22}^2)^T$ are so called control functions. These six control functions are completely defined by the adaptation mapping $\vec{s}^A : \mathcal{P}_{\xi\eta} \mapsto \mathcal{P}_{st}$.

The adapted grid in domain $\mathcal{D}$ is computed by first mapping the adapted boundary grid points at $\partial\mathcal{P}_{st}$ to the boundary of $\mathcal{D}$. Next, the interior adapted grid in $\mathcal{D}$ is computed by solving the Poisson system given by Eq.(13) with the already computed adapted grid points at the boundary of $\mathcal{D}$ as Dirichlet boundary conditions.

Grid adaptation in $\mathcal{P}_{st}$ may be based on solving the Laplace-Beltrami equations on a monitor surface given by

$$\vec{Q}(s,t) = (s, t, Q^1_{\mathcal{P}_{st}}(s,t), \ldots, Q^n_{\mathcal{P}_{st}}(s,t))^T, \tag{17}$$

where $(Q^1_{\mathcal{P}_{st}}(s,t), \ldots, Q^n_{\mathcal{P}_{st}}(s,t))^T = \vec{Q}_{\mathcal{P}_{st}}$ are the $n$ components of the normalized solution vector in $\mathcal{P}_{st}$. Let $\vec{\xi}^A : \mathcal{P}_{st} \mapsto \mathcal{P}_{\xi\eta}$ be the inverse of the adaptation mapping $\vec{s}^A : \mathcal{P}_{\xi\eta} \mapsto \mathcal{P}_{st}$. The two components of $\vec{\xi}^A : \mathcal{P}_{st} \mapsto \mathcal{P}_{\xi\eta}$, given by $\xi = \xi^A(s,t)$ and $\eta = \eta^A(s,t)$, must obey

$$\text{div } (M \text{ grad } \xi^A) = 0 \ , \ \text{div } (M \text{ grad } \eta^A) = 0, \tag{18}$$

where the matrix $M = M(s,t)$ is defined by Eq.(7). The two covariant base vectors are given by

$$\vec{a}_1 = \frac{\partial \vec{Q}}{\partial s} = \vec{Q}_s = (1, 0, \frac{\partial Q^1_{\mathcal{P}_{st}}}{\partial s}, \ldots, \frac{\partial Q^n_{\mathcal{P}_{st}}}{\partial s})^T, \tag{19}$$

$$\vec{a}_2 = \frac{\partial \vec{Q}}{\partial t} = \vec{Q}_t = (0, 1, \frac{\partial Q^1_{\mathcal{P}_{st}}}{\partial t}, \ldots, \frac{\partial Q^n_{\mathcal{P}_{st}}}{\partial t})^T. \tag{20}$$

According to Eq.(11) and Eq.(12), the natural boundary conditions at edge $E_1$ $(E_2)$ and edge $E_3$

$(E_4)$ become respectively

$$\eta_s^A = \frac{(\vec{Q}_s, \vec{Q}_t)}{(\vec{Q}_t, \vec{Q}_t)} \eta_t^A \ , \ \xi_t^A = \frac{(\vec{Q}_s, \vec{Q}_t)}{(\vec{Q}_s, \vec{Q}_s)} \xi_s^A. \tag{21}$$

Natural boundary conditions are such that the adapted grid is orthogonal at the boundary of the monitor surface. Sometimes it is desired that the adapted grid is orthogonal at the boundary of the domain $\mathcal{D}$ itself. Especially for Navier-Stokes computations, the orthogonality of the grid in a boundary-layer is often desired. The boundary conditions for grid orthogonality at the boundary of domain $\mathcal{D}$, which we call Neumann boundary conditions, is given by Eq.(21) with $\vec{Q}$ replaced by $\vec{x}$ where $\vec{x} : \mathcal{P}_{st} \mapsto \mathcal{D}$ is the elliptic transformation.

## 4 Numerical aspects

Eq.(18), supplied with the boundary conditions, can be solved on a non-uniform mesh in parameter space $\mathcal{P}_{st}$ to find $\vec{\xi}^A : \mathcal{P}_{st} \mapsto \mathcal{P}_{\xi\eta}$. However, from a numerical point of view this is not the easiest way to do. The solution of the Laplace-Beltrami equation on a monitor surface, only depends on the shape of the surface and the boundary conditions, but is independent of the parametrization of the surface. Thus the only information needed to compute the discrete solution of the Laplace-Beltrami equation, supplied with the boundary condition, are the locations of the grid points on the monitor surface. Thus, in practice, for a grid of $(N+1) \times (M+1)$ points on a monitor surface, point index coordinates $\{(i,j) \mid i = 0 \ldots N, j = 0 \ldots M\}$ are used as parametrization.

Consider the initial non-uniform grid in parameter space $\mathcal{P}_{st}$, given by the mapping $\vec{s}^I : \mathcal{P}_{\xi\eta} \mapsto \mathcal{P}_{st}$. Write this grid as $\{(s^I_{ij}, t^I_{ij}) \mid i = 0 \ldots N, j = 0 \ldots M\}$. The adapted grid in $\mathcal{P}_{st}$, given by the mapping $\vec{s}^A : \mathcal{P}_{\xi\eta} \mapsto \mathcal{P}_{st}$, and written as $\{(s^A_{ij}, t^A_{ij}) \mid i = 0 \ldots N, j = 0 \ldots M\}$, must be found by numerical inversion of the mapping $\vec{\xi}^A : \mathcal{P}_{st} \mapsto \mathcal{P}_{\xi\eta}$. This is done as follows. Let $\{(\xi^A_{ij}, \eta^A_{ij}) \mid i = 0 \ldots N, j = 0 \ldots M\}$ be the solution of the Laplace-Beltrami equation. Consider this grid as a non-overlapping subdivision of the computational space $\mathcal{P}_{\xi\eta}$ by $N \times M$ patches, where each patch has four corner points. For a given grid point $(i,j)$ of the uniform grid in $\mathcal{P}_{\xi\eta}$, given by $(\xi_{ij}, \eta_{ij}) = (i/N, j/M)$ the corresponding grid point $(s^A_{ij}, t^A_{ij})$ of the adapted grid is obtained as follows. Suppose that $(\xi_{ij}, \eta_{ij})$ belongs to patch (p,q) as shown in Fig.26.

The local patch parameters $\alpha$ and $\beta$ are now defined by the following two bilinear equations

$$\begin{aligned}
\xi_{i,j} &= \xi^A_{p,q}(1-\alpha)(1-\beta) + \xi^A_{p+1,q}\alpha(1-\beta) + \xi^A_{p,q+1}(1-\alpha)\beta + \xi^A_{p+1,q+1}\alpha\beta, \\
\eta_{i,j} &= \eta^A_{p,q}(1-\alpha)(1-\beta) + \eta^A_{p+1,q}\alpha(1-\beta) + \eta^A_{p,q+1}(1-\alpha)\beta + \eta^A_{p+1,q+1}\alpha\beta.
\end{aligned}$$

The two parameters $\alpha$ and $\beta$ are solved by Newton iteration. Note that $0 \leq \alpha \leq 1$ and $0 \leq \beta \leq 1$ because $(\xi_{ij}, \eta_{ij})$ belongs to patch (p,q). After computation of $\alpha$ and $\beta$, a corresponding grid point $(s^A_{ij}, t^A_{ij})$ of the adapted grid is given by

$$\begin{aligned}
s^A_{i,j} &= s^I_{p,q}(1-\alpha)(1-\beta) + s^I_{p+1,q}\alpha(1-\beta) + s^I_{p,q+1}(1-\alpha)\beta + s^I_{p+1,q+1}\alpha\beta, \\
t^A_{i,j} &= t^I_{p,q}(1-\alpha)(1-\beta) + t^I_{p+1,q}\alpha(1-\beta) + t^I_{p,q+1}(1-\alpha)\beta + t^I_{p+1,q+1}\alpha\beta.
\end{aligned}$$

After one adaptation step, we obtain a new adapted grid $\{(s^A_{ij}, t^A_{ij}) \mid i = 0 \ldots N, j = 0 \ldots M\}$ in parameter space $\mathcal{P}_{st}$. This grid can be considered as a new initial grid in $\mathcal{P}_{st}$ on which a next

adaptation step can be performed. Assume that the monitor surface function does not change during adaptation. The components of the monitor surface are recomputed on this new grid and the process can be repeated until convergence is reached. Convergence is obtained when $\{(\xi_{ij}^A, \eta_{ij}^A) = (\xi_{ij}, \eta_{ij}) = (i/N, j/M) \;\; | \;\; i = 0 \ldots N, j = 0 \ldots M\}$. In practice, about 5-10 adaptation steps are sufficient to reach convergence.

If the solution vector $\vec{Q}_{\mathcal{P}_{st}}$ is constant, then the matrix $M = M(s,t)$ is the unit matrix and the Laplace-Beltrami equations, Eq.(18), simplify to the Laplace equations: $\triangle \xi^A = \xi_{ss}^A + \xi_{tt}^A = 0$ and $\triangle \eta^A = \eta_{ss}^A + \eta_{tt}^A = 0$. Thus after adaptation, we will get a uniform grid in $\mathcal{P}_{st}$. Consequently, the adapted grid in domain $\mathcal{D}$ becomes a Laplace grid so that all features of the initial grid will get lost. From a practical point of view, this behavior is unwanted. Instead, it is much more desirable that an initial grid remains unchanged when the solution vector is constant. This can be achieved by redefining the monitor surface, given by Eq.(17), as

$$\vec{Q}(s,t) = (\xi^I(s,t), \eta^I(s,t), Q^1_{\mathcal{P}_{st}}(s,t), \ldots, Q^n_{\mathcal{P}_{st}}(s,t))^T, \tag{22}$$

where $\vec{\xi}^I : \mathcal{P}_{st} \mapsto \mathcal{P}_{\xi\eta}$ is the inverse of the mapping $\vec{s}^I : \mathcal{P}_{\xi\eta} \mapsto \mathcal{P}_{st}$. In that case, if $\vec{Q}_{\mathcal{P}_{st}}$ is constant, the matrix $M = M(s,t)$ becomes

$$M = \frac{1}{\xi_s^I \eta_t^I - \xi_t^I \eta_s^I} \begin{pmatrix} (\xi_t^I)^2 + (\eta_t^I)^2 & -(\xi_s^I \xi_t^I + \eta_s^I \eta_t^I) \\ -(\xi_s^I \xi_t^I + \eta_s^I \eta_t^I) & (\xi_s^I)^2 + (\eta_s^I)^2 \end{pmatrix}. \tag{23}$$

Then $M$ grad $\xi^I = (\eta_t^I, -\eta_s^I)^T$ and $M$ grad $\eta^I = (-\xi_t^I, \xi_s^I)^T$, so that div $(M$ grad $\xi^I)$ $= 0$ and div $(M$ grad $\eta^I) = 0$. Thus, in that case, the mapping $\vec{\xi}^I : \mathcal{P}_{st} \mapsto \mathcal{P}_{\xi\eta}$ already obeys the Laplace-Beltrami equations and the initial grid will therefore remain unchanged during adaptation.

If Eq.(22) is used for the definition of the monitor surface, then, during the first adaptation step, the Laplace-Beltrami equations are in fact solved on a uniform mesh in a parameter space. Then the method resembles the approach of Hagmeijer, Ref. 3, who used anisotropic diffusion equations instead of Laplace-Beltrami equations on uniforms grids in a parametric domain.

## 5 Illustrations

Only grid adaptation in parameter space $\mathcal{P}_{st}$ is considered. The mapping of the adapted grid into a domain $\mathcal{D}$, based on the Poisson system given by Eq.(13), is not shown.

In all cases, the initial grid in $\mathcal{P}_{st}$ is uniform, so that there is no distinction between the definition of the monitor surface function defined by Eq.(17) and Eq.(22). All adapted grids are converged solutions obtained after 5-10 adaptation steps.

Fig.2 through Fig.9 show adaptive grids for a scalar monitor function defined as $Q_{\mathcal{P}_{st}}(s,t) = \alpha\ tanh(80(1/16-(s-1/2)^2-(t-1/2)^2))$. As illustrated, the amount of adaptation can be varied by changing the height $\alpha$ of this "table" function.

Fig.10 through Fig.13 illustrate grid adaptation to a curved "shock". The example is based on a solution function borrowed from Ref. 5: $Q_{\mathcal{P}_{st}}(s,t) = tanh(5((5/4)^2-(s-3/2)^2-t^2))$. Natural boundary conditions are used. Fig.12 illustrates that the adapted grid is such that it uniformly covers the monitor surface with grid points.

Grid adaptation towards a parabola $Q^1_{\mathcal{P}_{st}}(s,t) = tanh(5(t-3(s-1/2)^2))$ is illustrated in Fig.14 through Fig.17. This example can also be found in Ref. 6. Fig.18 depicts the adapted grid towards the parabola $Q^1_{\mathcal{P}_{st}}$ and a straight-line $Q^2_{\mathcal{P}_{st}}(s,t) = tanh(5(t-s))$.

Fig.19 through Fig.24 shows an adaptation to a model problem that simulates the interaction of an oblique-shock and a boundary-layer as used in Ref. 3. The two components of the corresponding solution vector are defined as $Q^1_{\mathcal{P}_{st}}(s,t) = tanh(50t)$ and $Q^2_{\mathcal{P}_{st}}(s,t) = tanh(25(t-s+0.5)/\sqrt{2})$. $Q^1_{\mathcal{P}_{st}}$ is called the boundary-layer function and $Q^2_{\mathcal{P}_{st}}$ is called the shock function. The Neumann boundary condition is used at the edge where the boundary-layer is situated. Thus the grid lines of the adapted grid should be orthogonal at this edge. Natural boundary conditions are used at the other three edges. Fig.21 and Fig.22 illustrate that the adapted grid tries to uniformly cover both the monitor surface of the boundary-layer function and the shock function. The adapted grid is clearly a compromise between conflicting requirements. Fig.23 and Fig.24 show respectively the complete adapted grid and a blow-up at the foot of the shock. At the foot of the shock, the adapted grid is clearly orthogonal at the boundary. Fig.25 shows a blow-up of the adapted grid in the boundary-layer at a location left to the foot of the shock. In this region, the adapted grid uniformly covers the monitor surface of the boundary-layer function, as shown in Fig.21. Therefore, the skewness of the adapted grid in the boundary-layer is inherent to our approach and cannot be removed by only specifying a Neumann boundary condition. This is a severe problem, because in practice, grids

should be orthogonal in the complete boundary-layer and not only at the boundary of a domain. This problem also occurs in the approach of Hagmeijer Ref. 3, who solved the problem by introducing the MAD (Modified Anisotropic Diffusion) equations. Such an approach cannot be easily done with the Laplace-Beltrami equations, without loosing the mathematical rigour of the method.

## 6 Conclusions

Grid adaptation based on solving the Laplace-Beltrami equations on a monitor surface in parameter space, is a sound mathematical approach. The adapted grids clearly resolve the solution vector. However, the method provides no control about grid skewness, which appears to be a problem, especially in boundary-layers.

## 7 References

1. S.P. Spekreijse, Elliptic Grid Generation Based on Laplace Equations and Algebraic Transformations, J. Comput. Phys. 118, 38-61, 1995.
2. P.R. Eiseman, Adaptive Grid Generation, Computer Methods Appl. Mech. Eng. 64, 321-376, 1987.
3. R. Hagmeijer, Grid Adaptation Based on Modified Anisotropic Diffusion Equations Formulated in the Parametric Domain, J. Comput. Phys. 115, 169-183, 1994.
4. E. Kreyszig, Introduction to Differential Geometry and Riemannian Geometry, Mathematical Expositions no.16, University of Toronto Press,1967.
5. P.M. Knupp, Jacobian-Weighted Elliptic Grid Generation, to appear in Siam J. Sci. Comp.,1996.
6. A.S. Dvinsky, Adaptive Grid Generation from Harmonic Maps on Riemannian Manifolds, J. Comput. Phys. 95, 450-476, 1991.
7. J.U. Brackbill, An Adaptive Grid with Directional Control, J. Comput. Phys. 108, 38-50, 1993.
8. S.A. Ivanenko, Adaptive-Harmonic Grid Generator, in: Proceedings 5th Numerical Grid Generation in Computational Field Simulation, pp. 167-176, eds. B.K. Soni et. al., Mississippi, 1996.

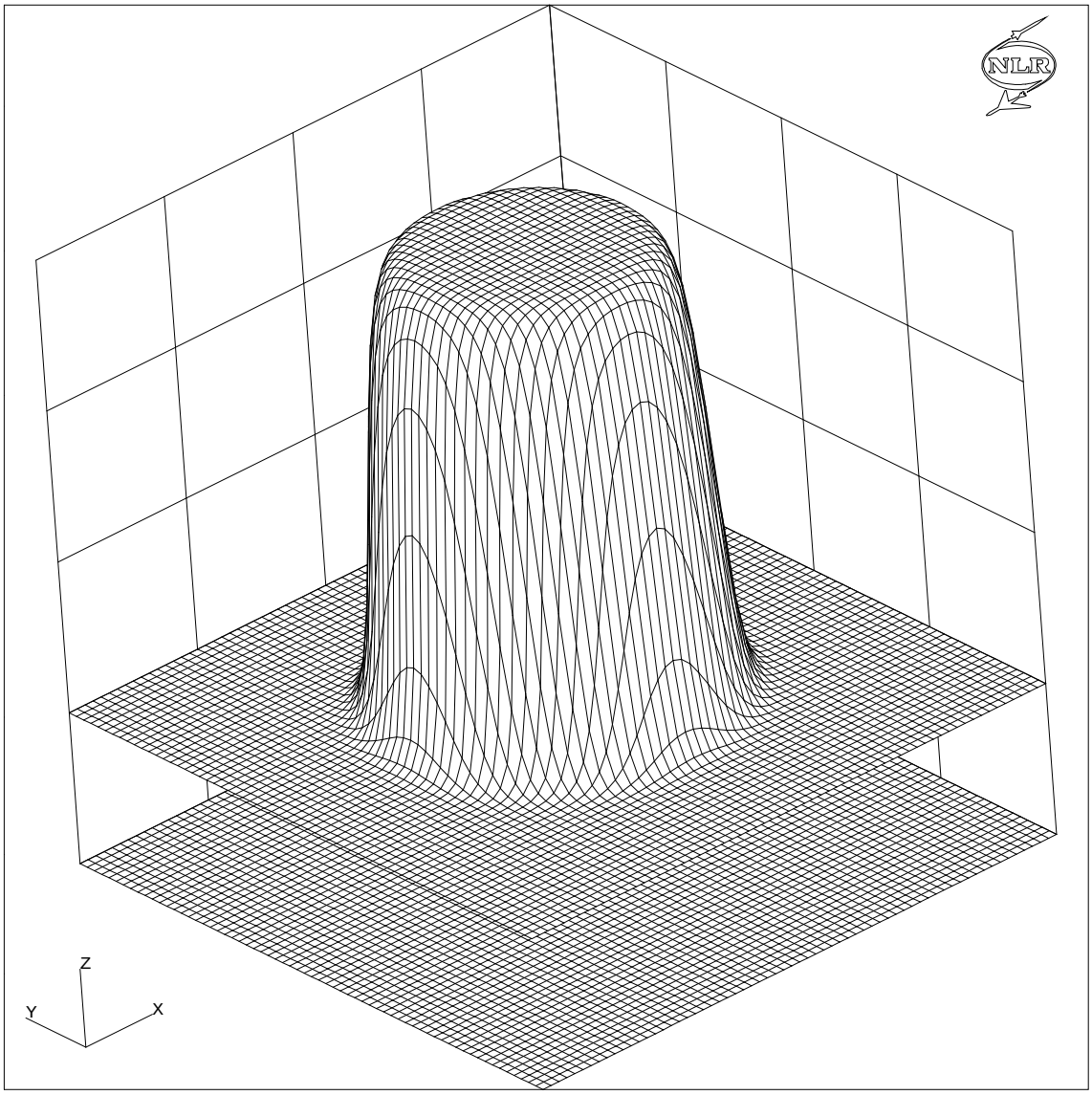


*Fig. 2 Monitor surface and initial grid of a "table" function:* $Q(s,t) = \alpha\ tanh(80(1/16 - (s - 1/2)^2 - (t - 1/2)^2))$. *The parameter* $\alpha$ *is used to vary the height.*

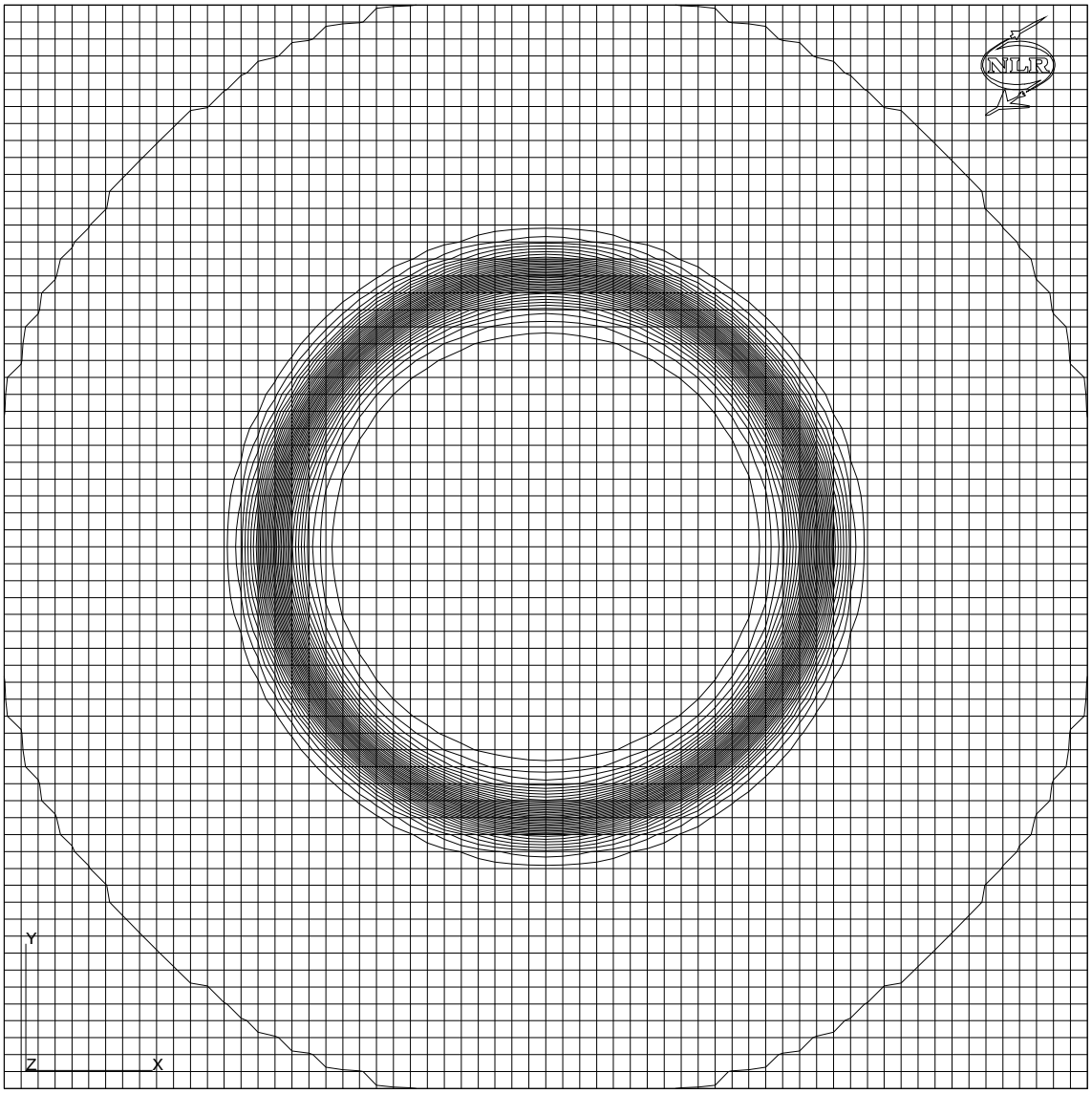


*Fig. 3 Contour-lines and initial grid.*

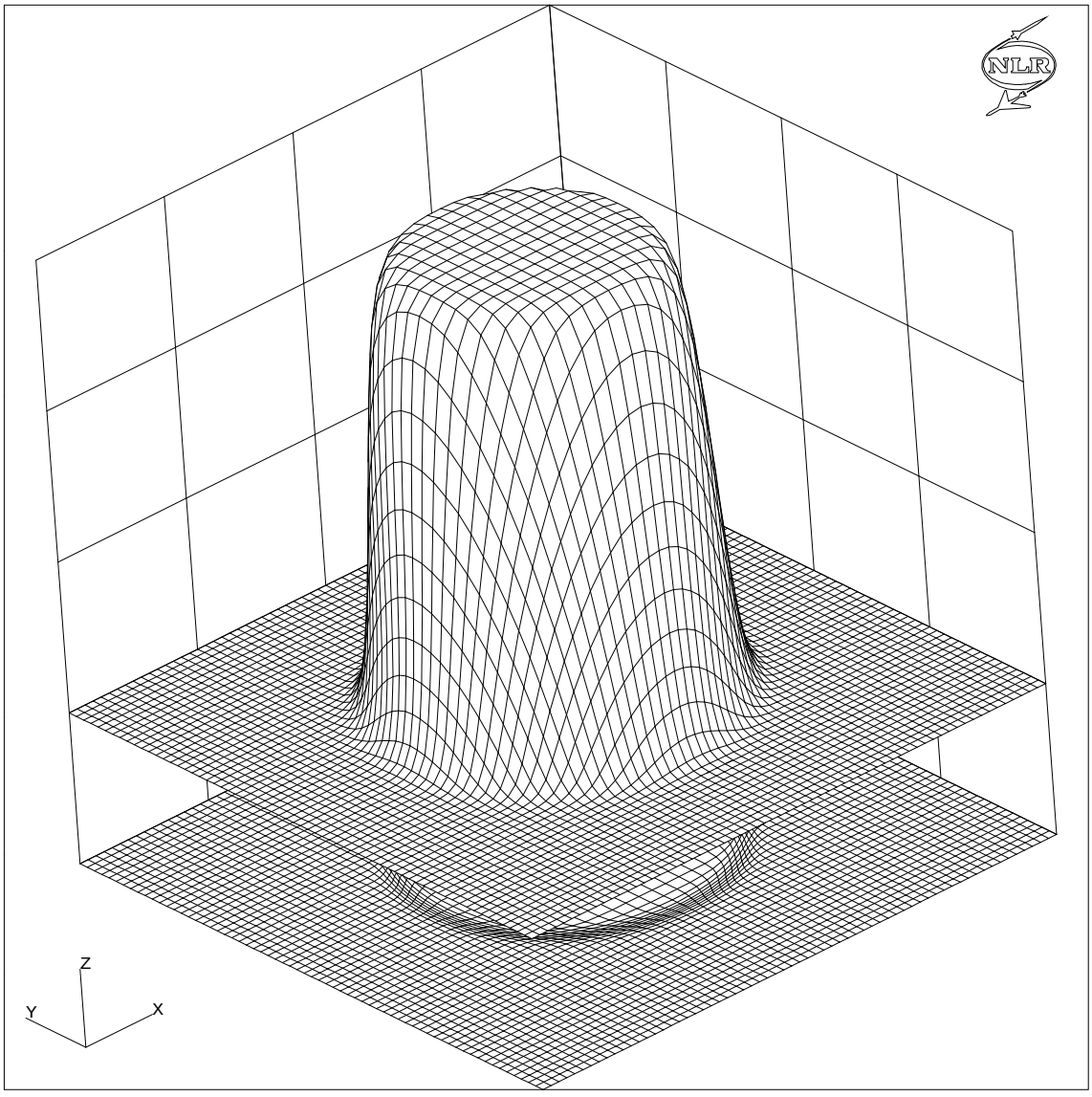


*Fig. 4 Monitor surface and adapted grid.*

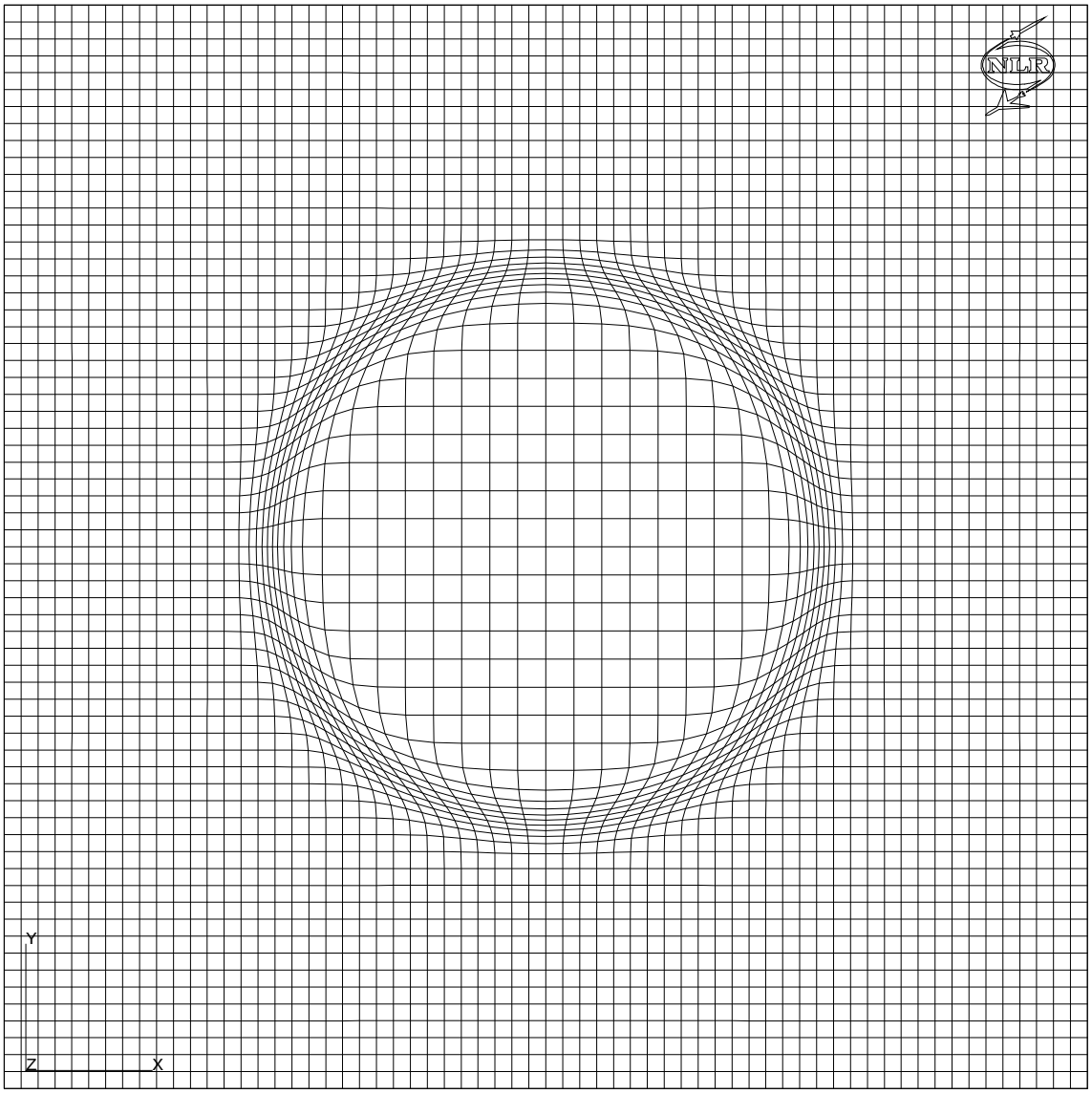


*Fig. 5 Adapted grid. The height of the table function is defined by the parameter* $\alpha = 0.1$.

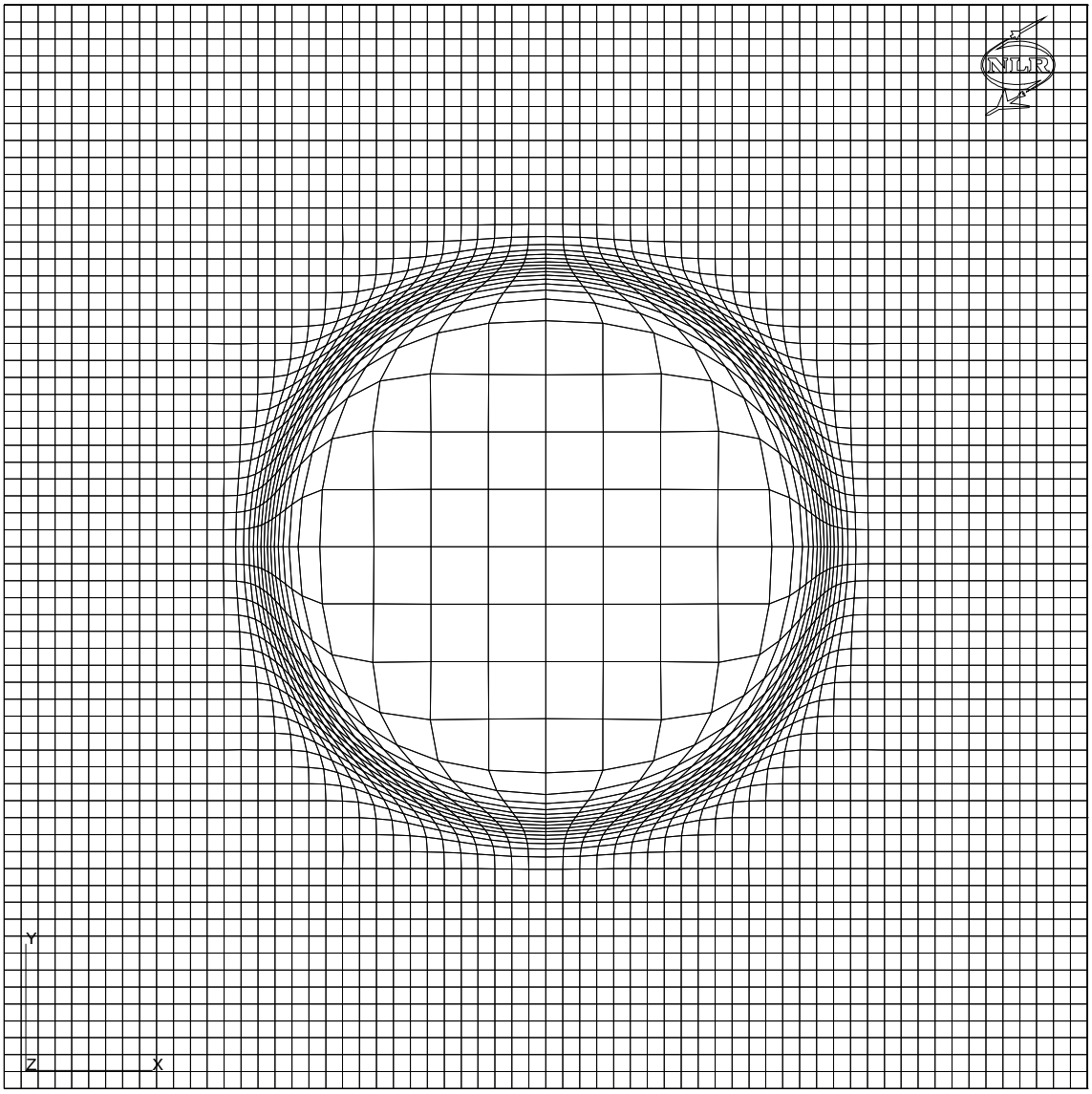


*Fig. 6 Adapted grid corresponding to an increase of the height of the table function ($\alpha = 0.2$).*

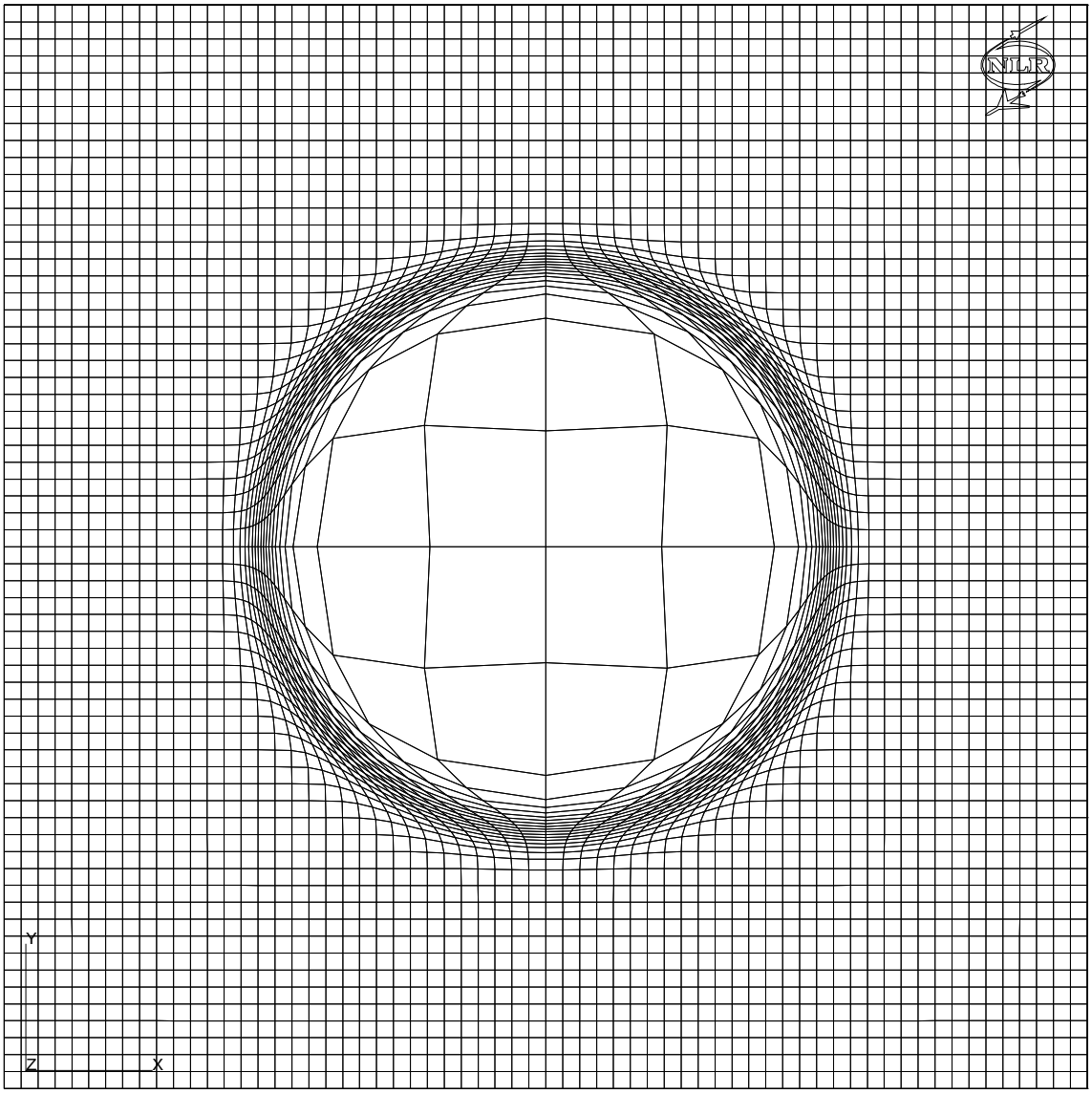


*Fig. 7 Adapted grid corresponding to an increase of the height of the table function ($\alpha = 0.3$).*

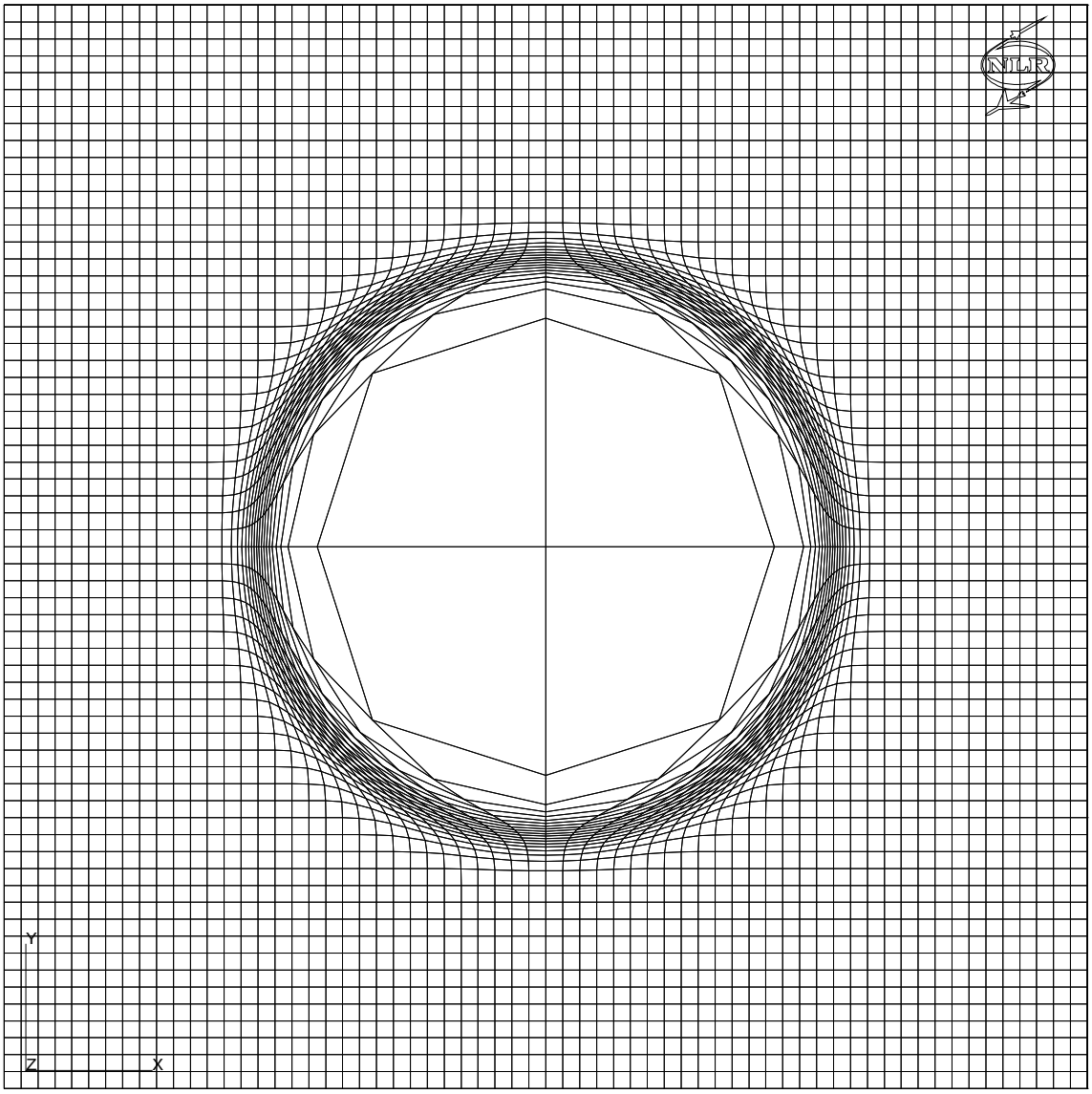


*Fig. 8 Adapted grid corresponding to an increase of the height of the table function ($\alpha = 0.4$).*

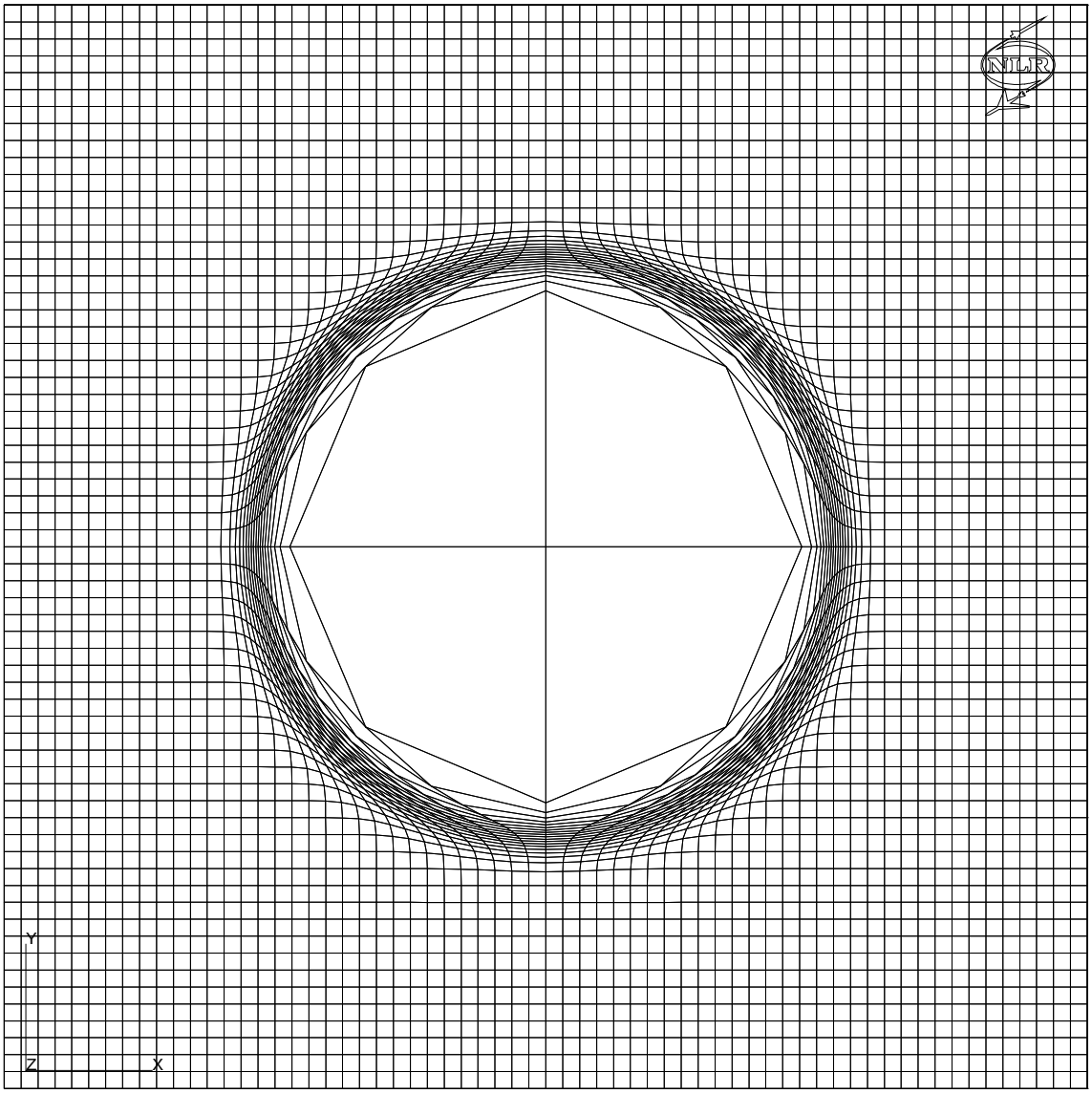


*Fig. 9 Adapted grid corresponding to an increase of the height of the table function ($\alpha = 0.5$).*

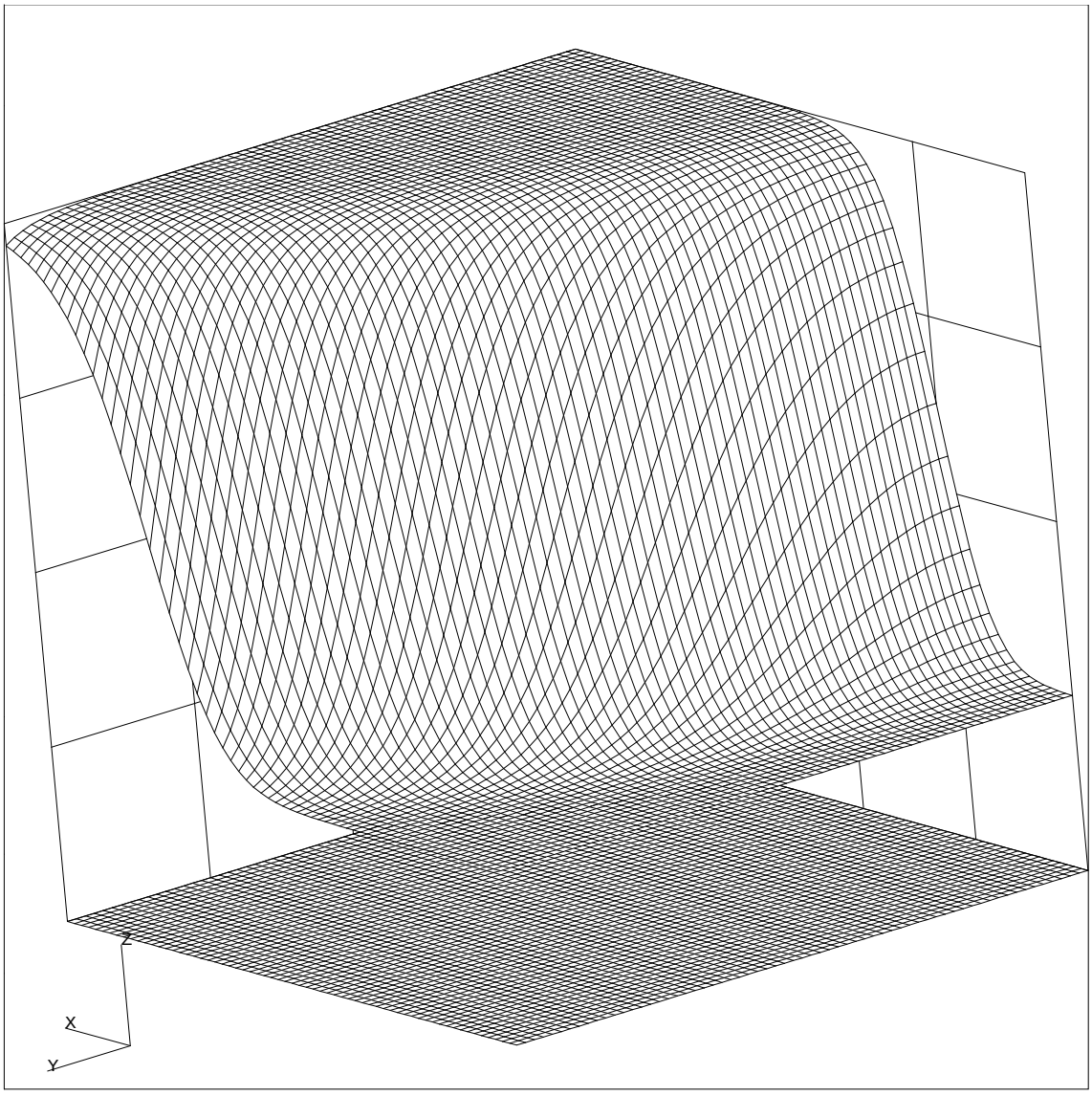


*Fig. 10 Monitor surface and initial grid of a curved "shock":* $Q(s,t) = tanh(5((5/4)^2 - (s - 3/2)^2 - t^2))$.

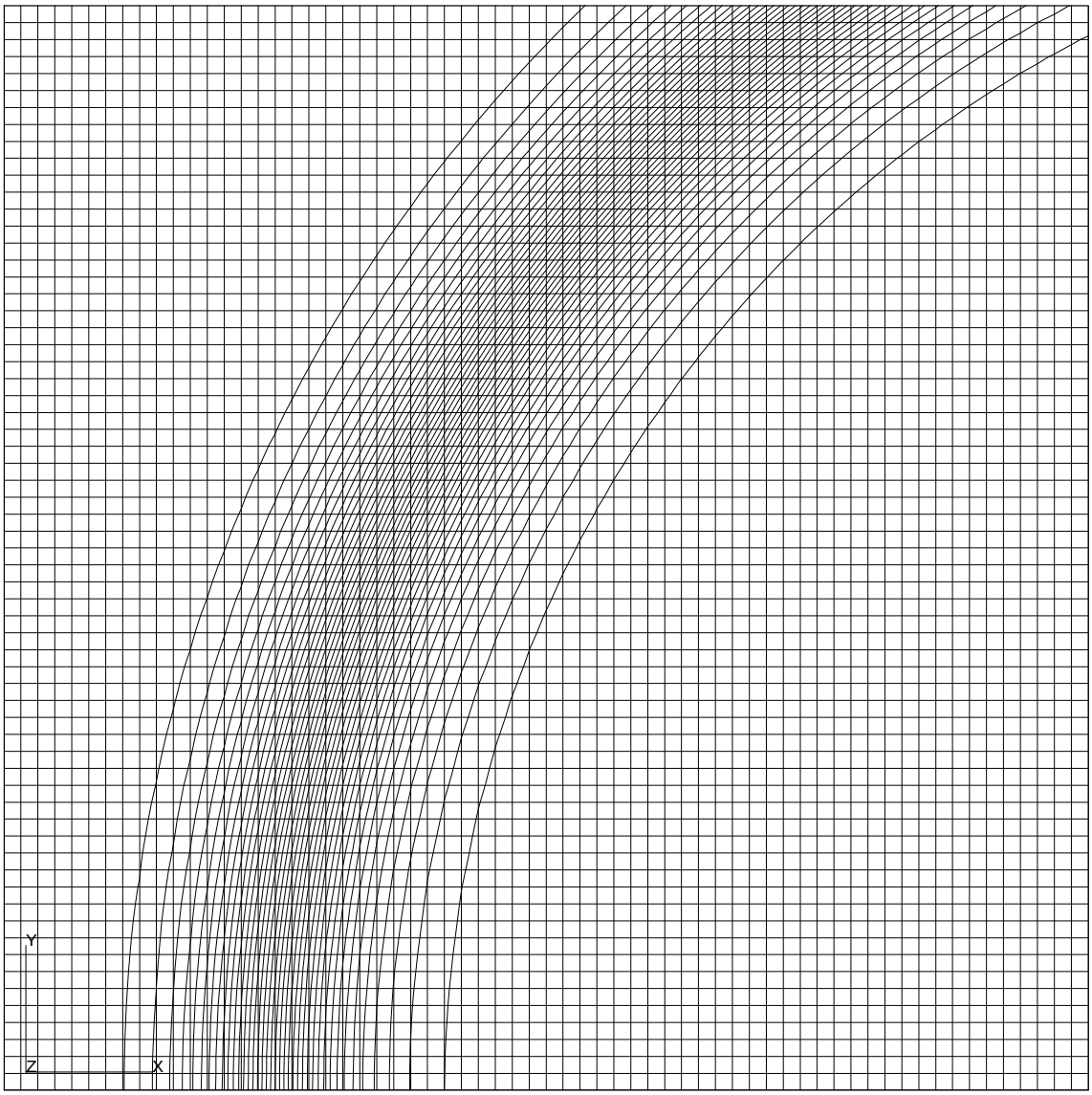


*Fig. 11 Contour-lines and initial grid.*

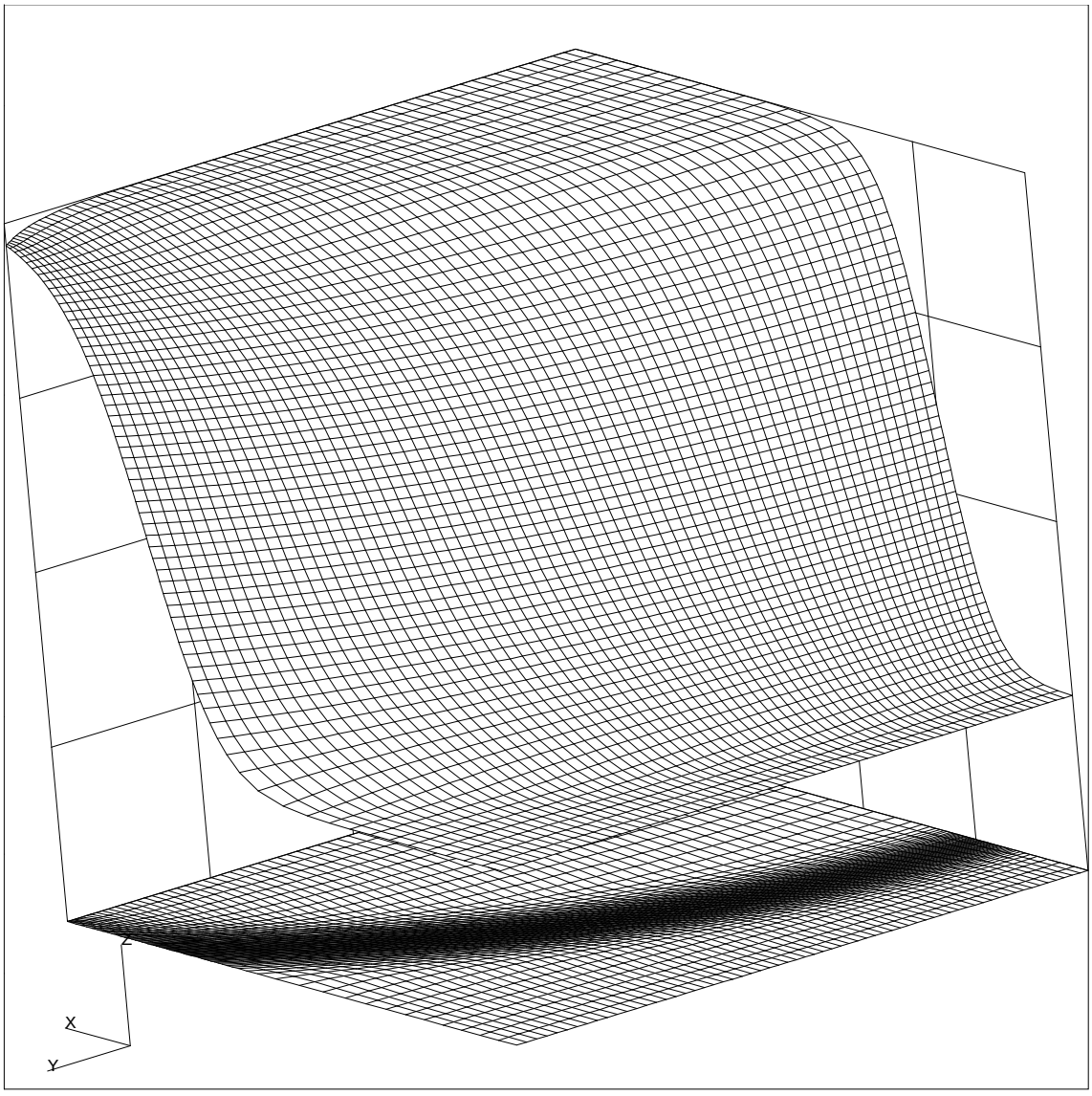


*Fig. 12 Monitor surface and adapted grid.*

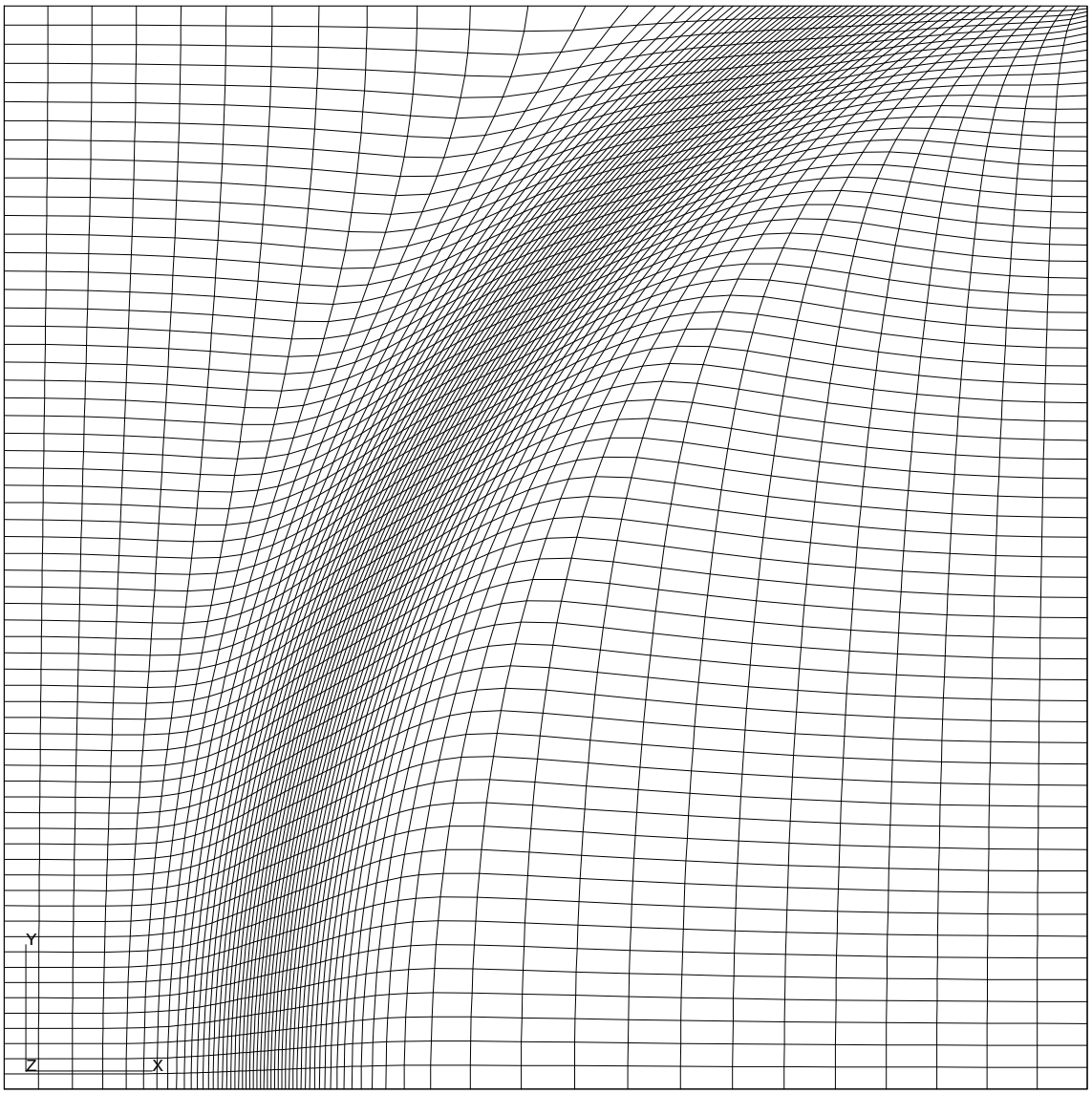


*Fig. 13 Adapted grid.*

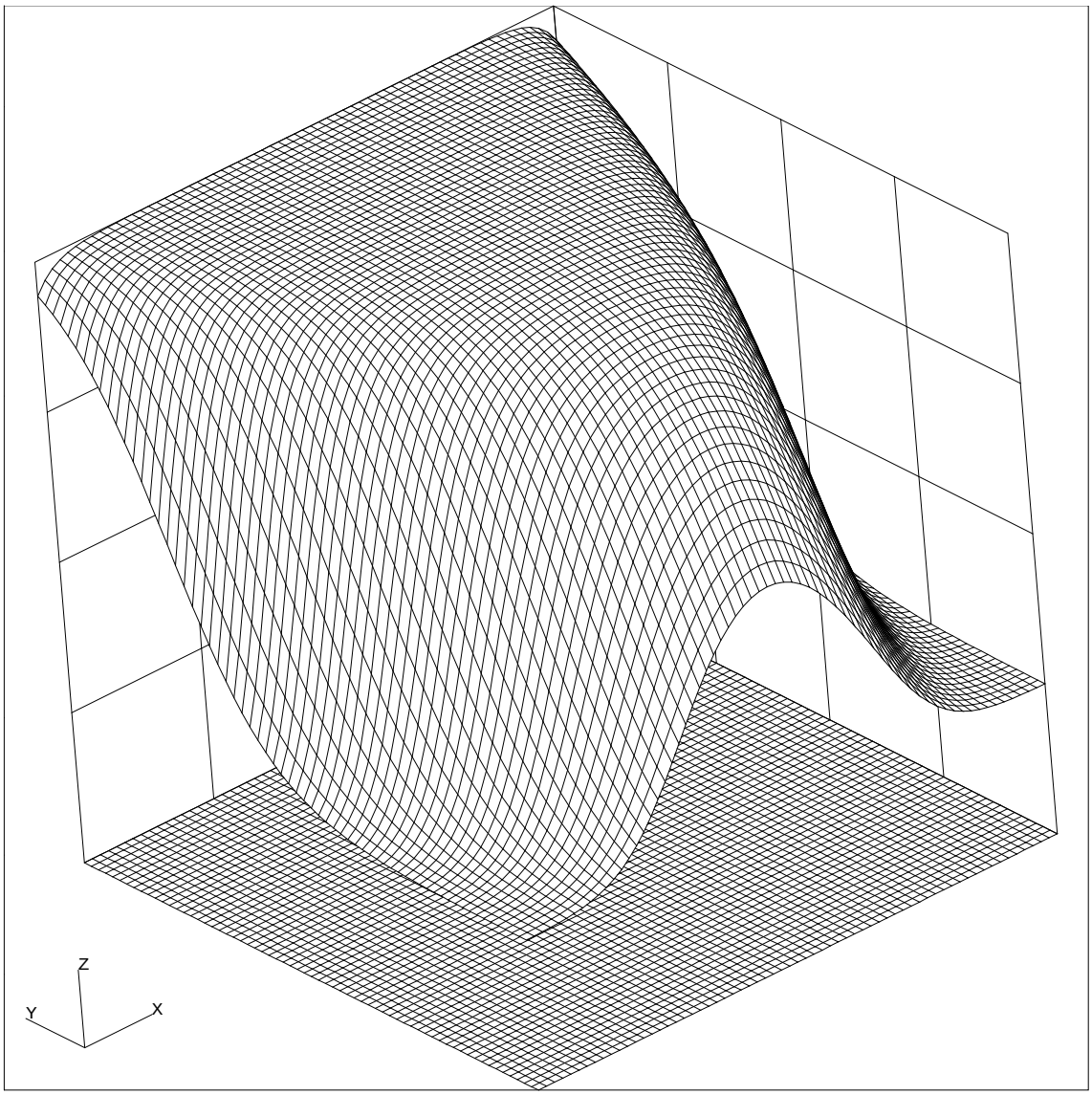


*Fig. 14 Monitor surface and initial grid of a parabola:* $Q(s,t) = tanh(5(t - 3(s - 1/2)^2))$.

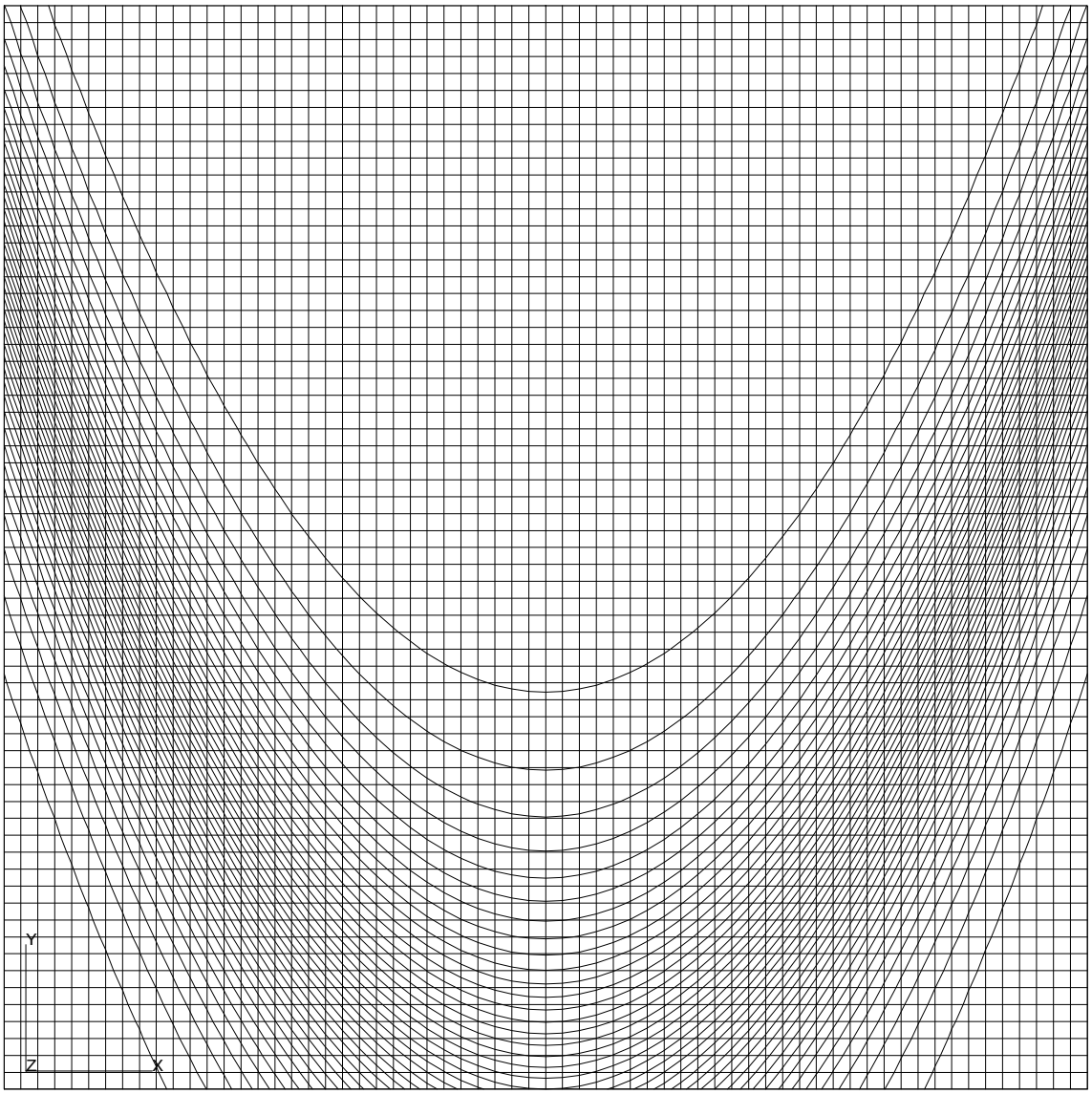


*Fig. 15 Contour-lines and initial grid.*

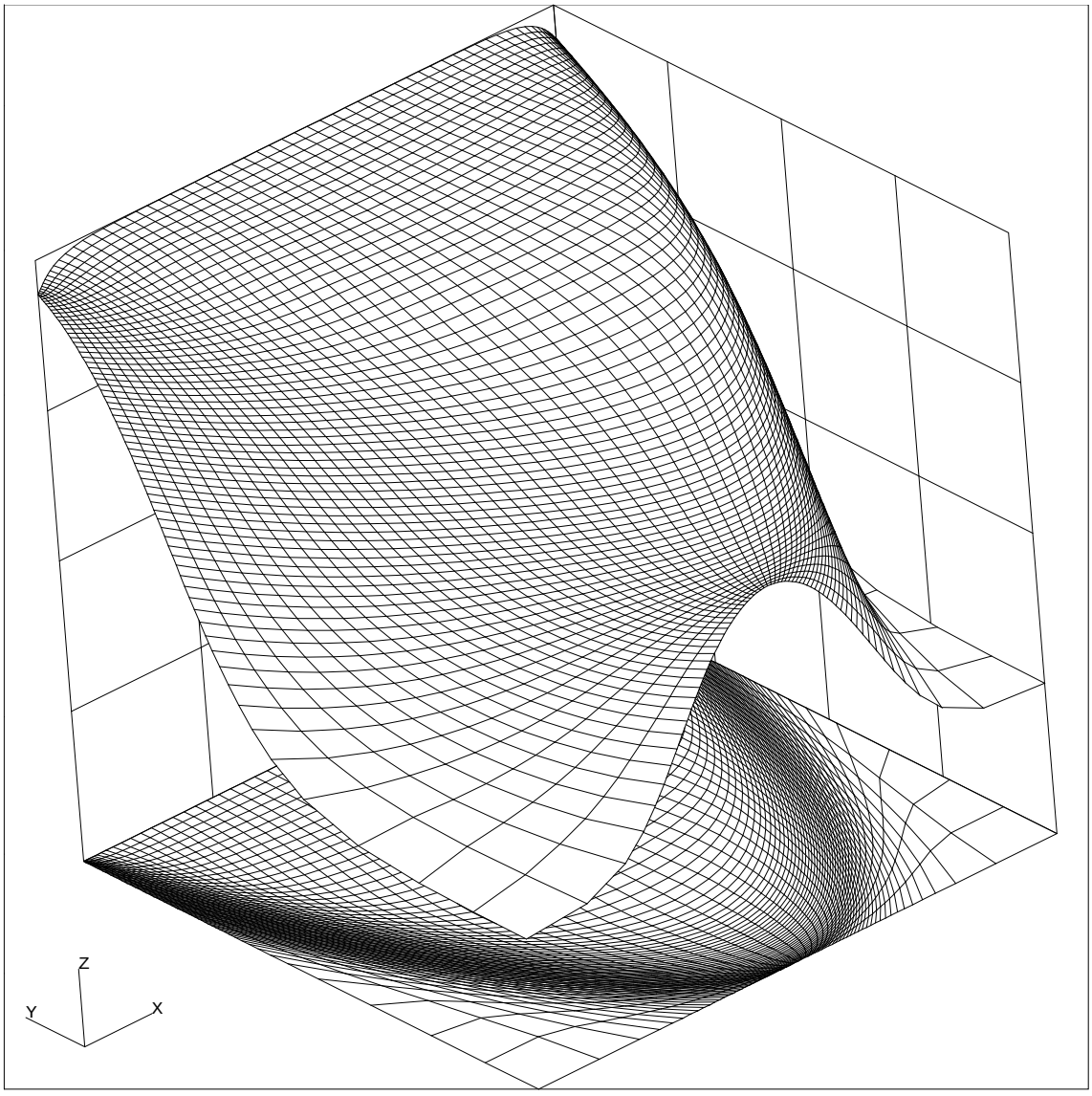


*Fig. 16 Monitor surface and adapted grid.*

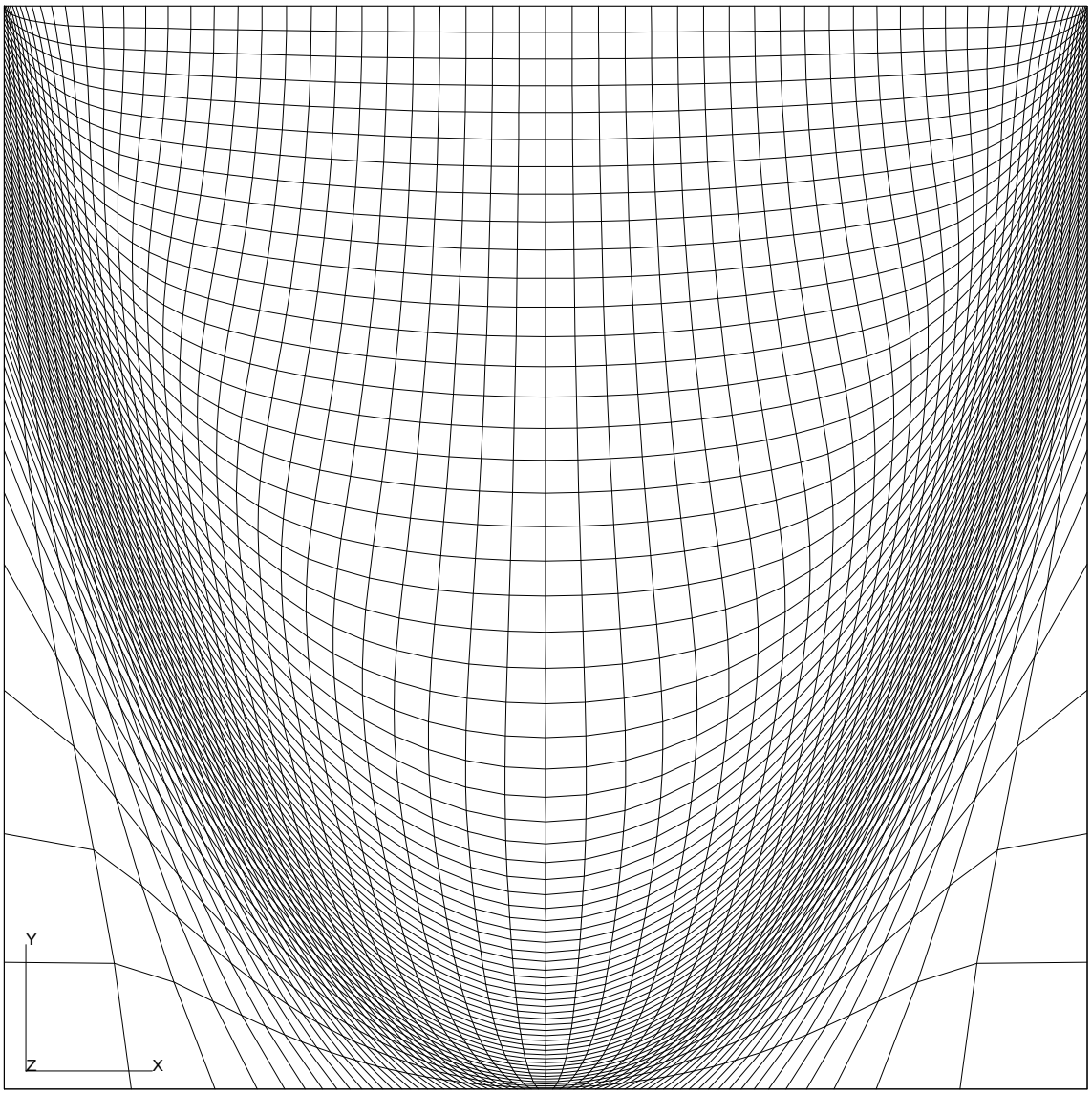


*Fig. 17 Adapted grid.*

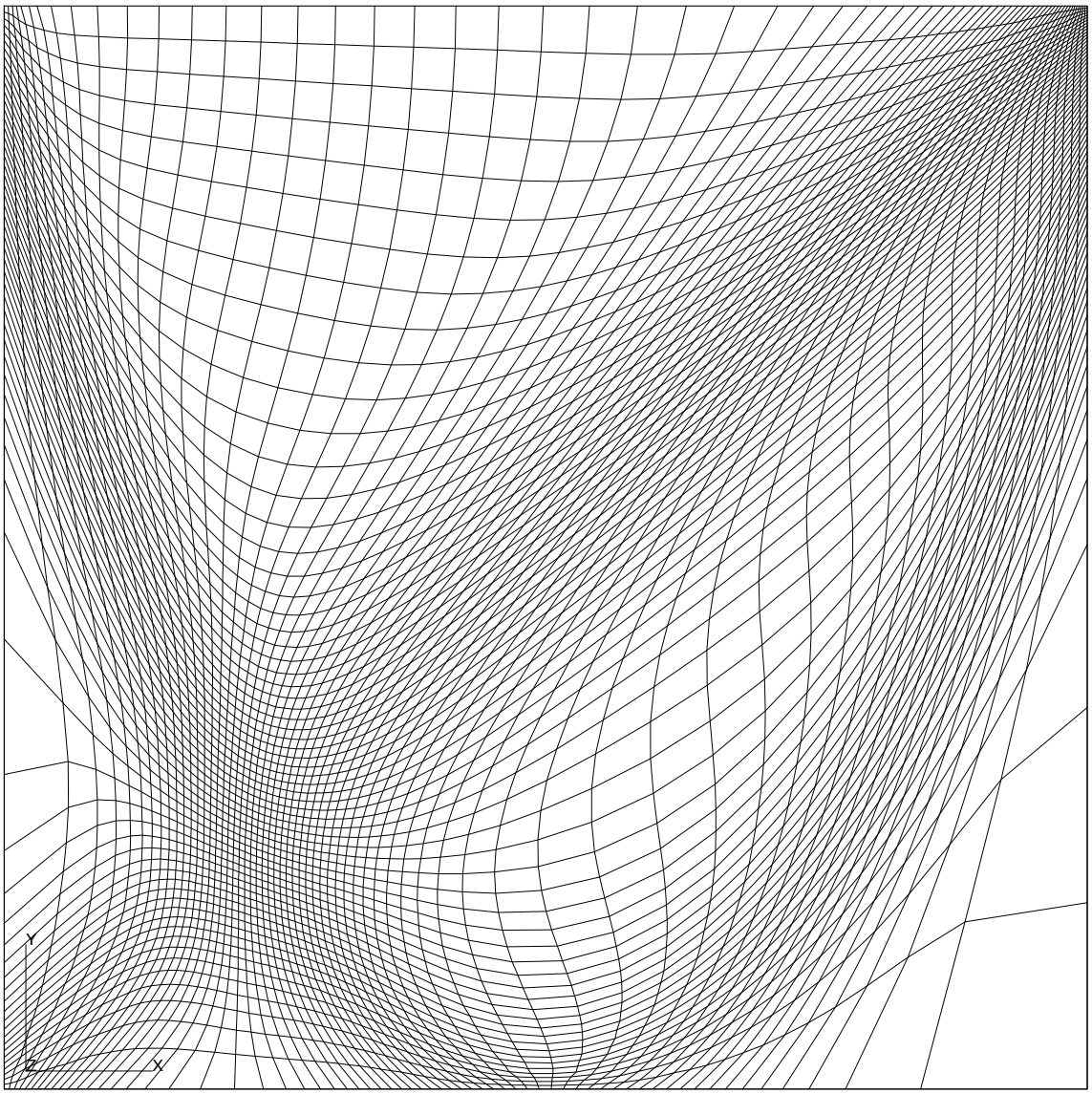


*Fig. 18 Adapted grid to a parabola:* $Q^1(s,t) = tanh(5(t - 3(s - 1/2)^2))$*, and a straight-line:* $Q^2(s,t) = tanh(5(t - s))$.

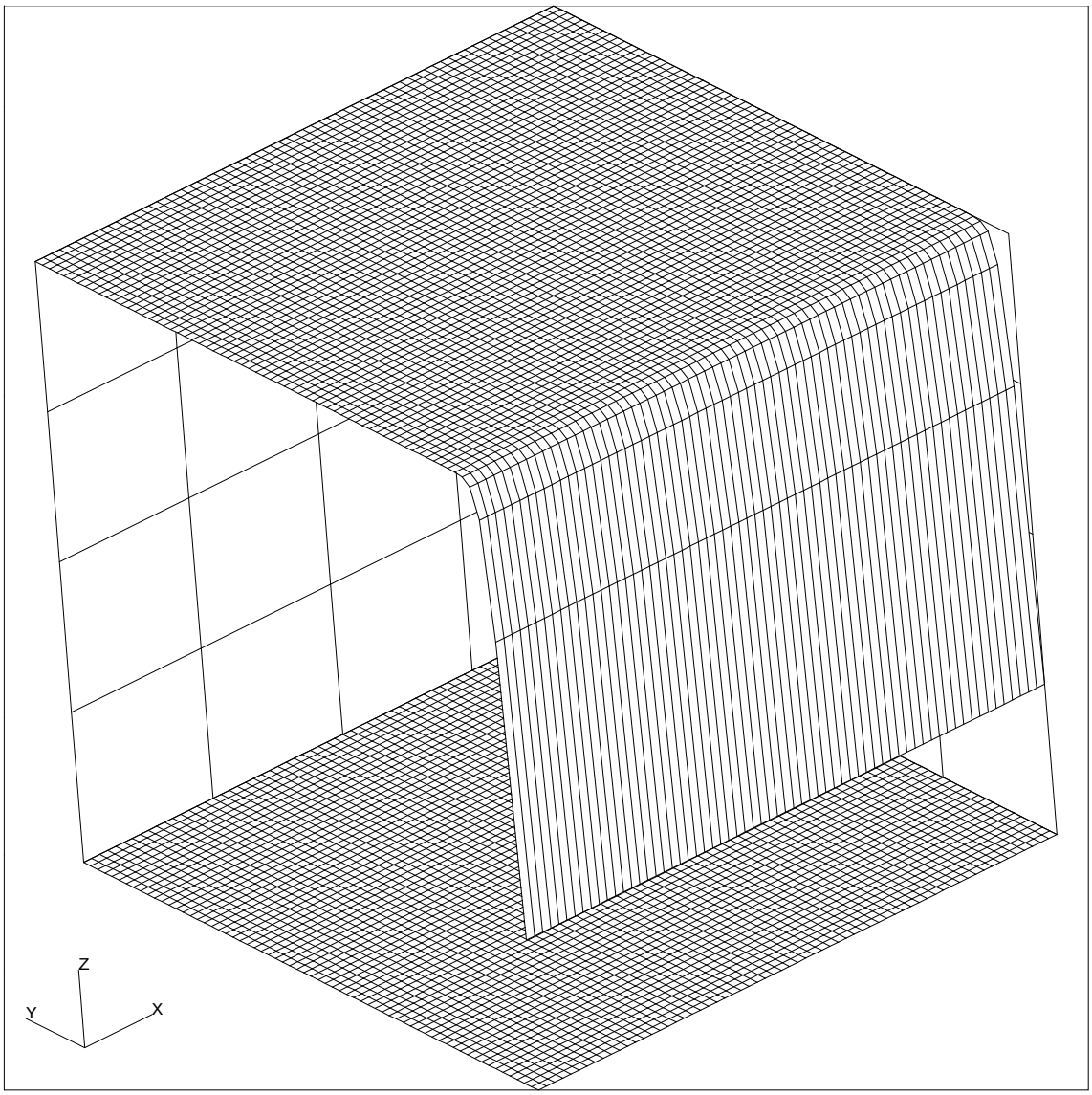


*Fig. 19 Initial grid and monitor surface of boundary-layer function:* $Q^1(s,t) = tanh(50t)$.

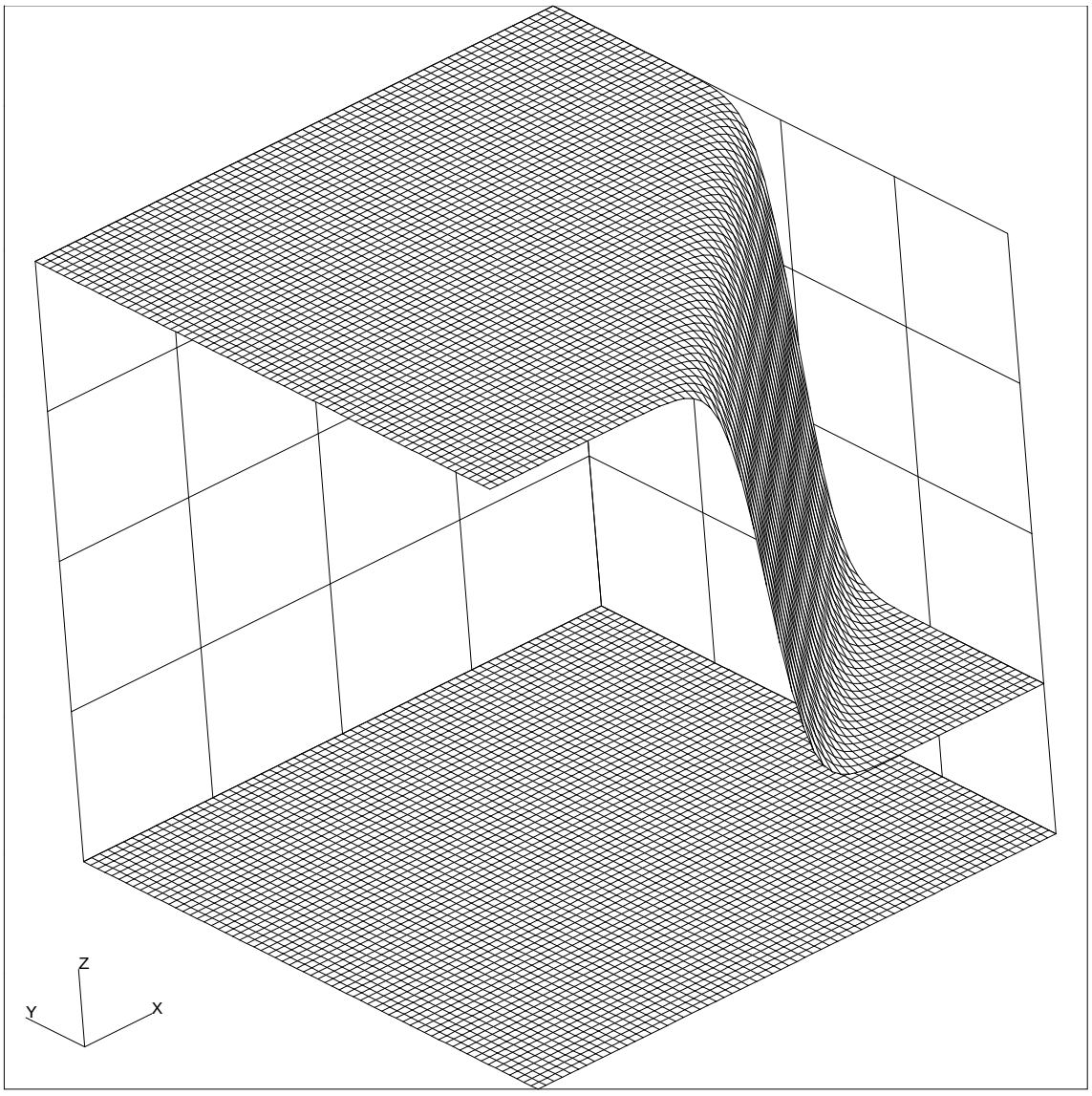


*Fig. 20 Initial grid and monitor surface of an oblique shock function:* $Q^2(s,t) = tanh(25(t - s + 0.5)/\sqrt{2})$.

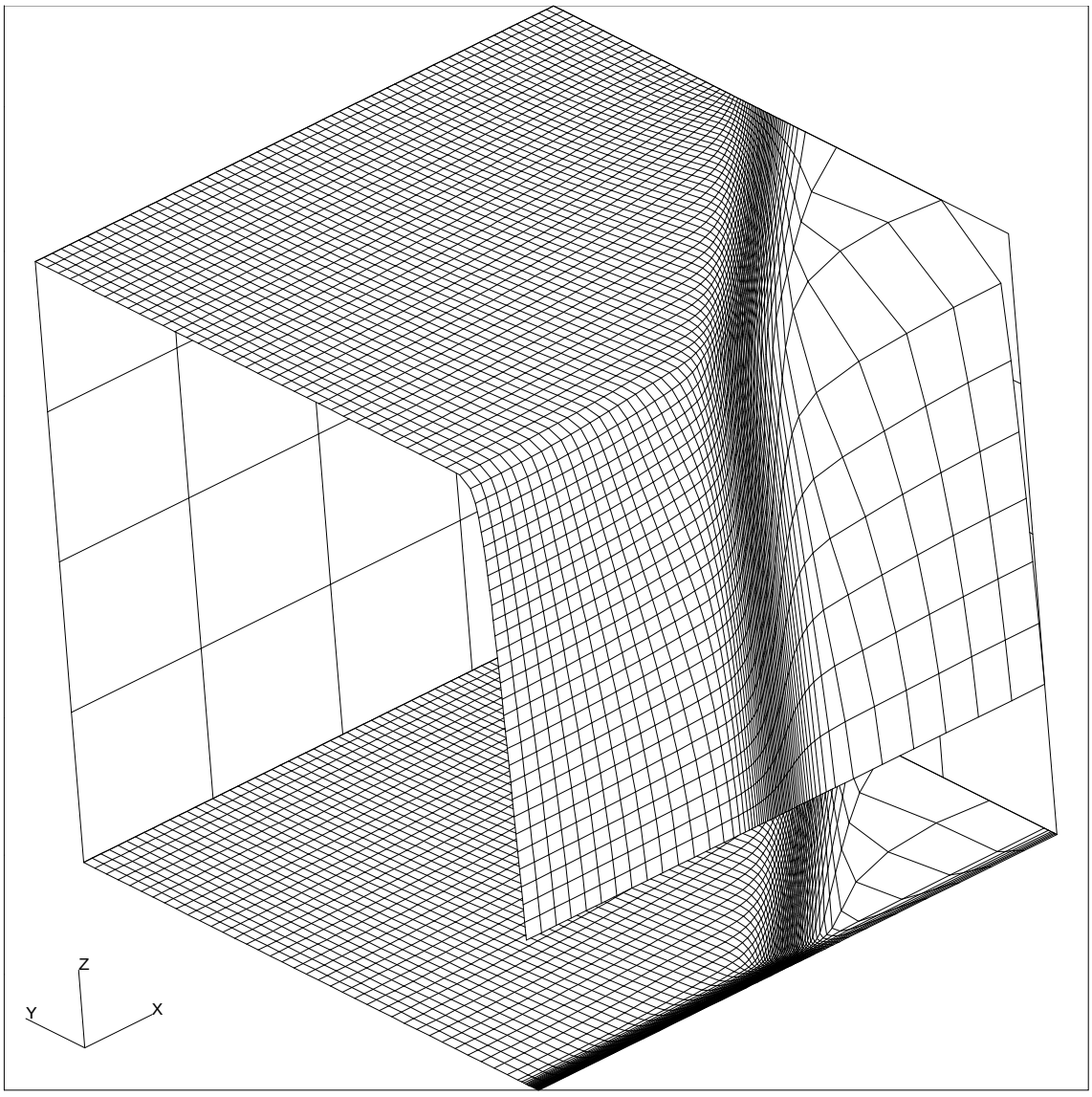


*Fig. 21 Adapted grid and monitor surface of boundary-layer function.*

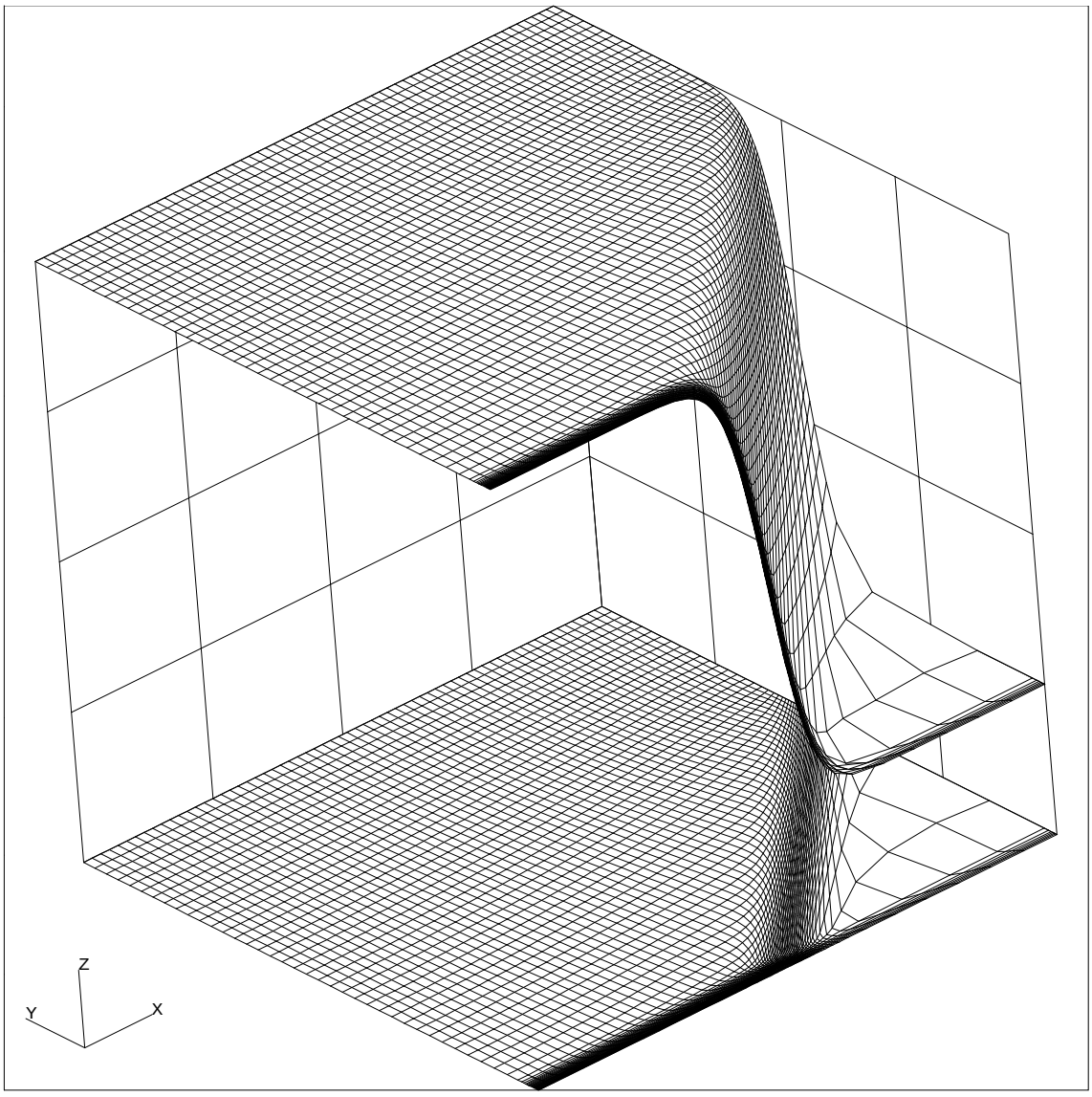


*Fig. 22 Adapted grid and monitor surface of shock function.*

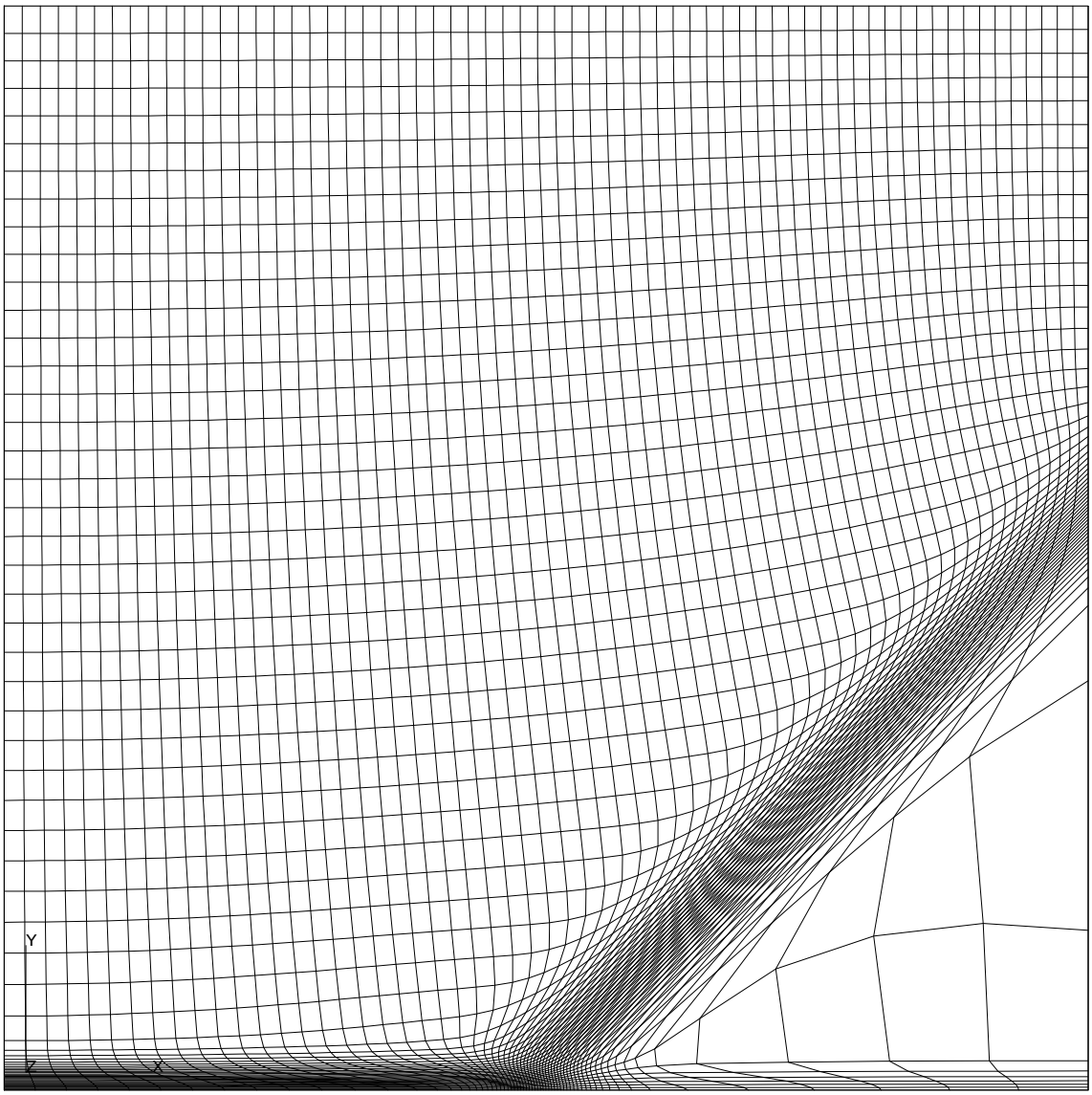


*Fig. 23 Adapted grid.*

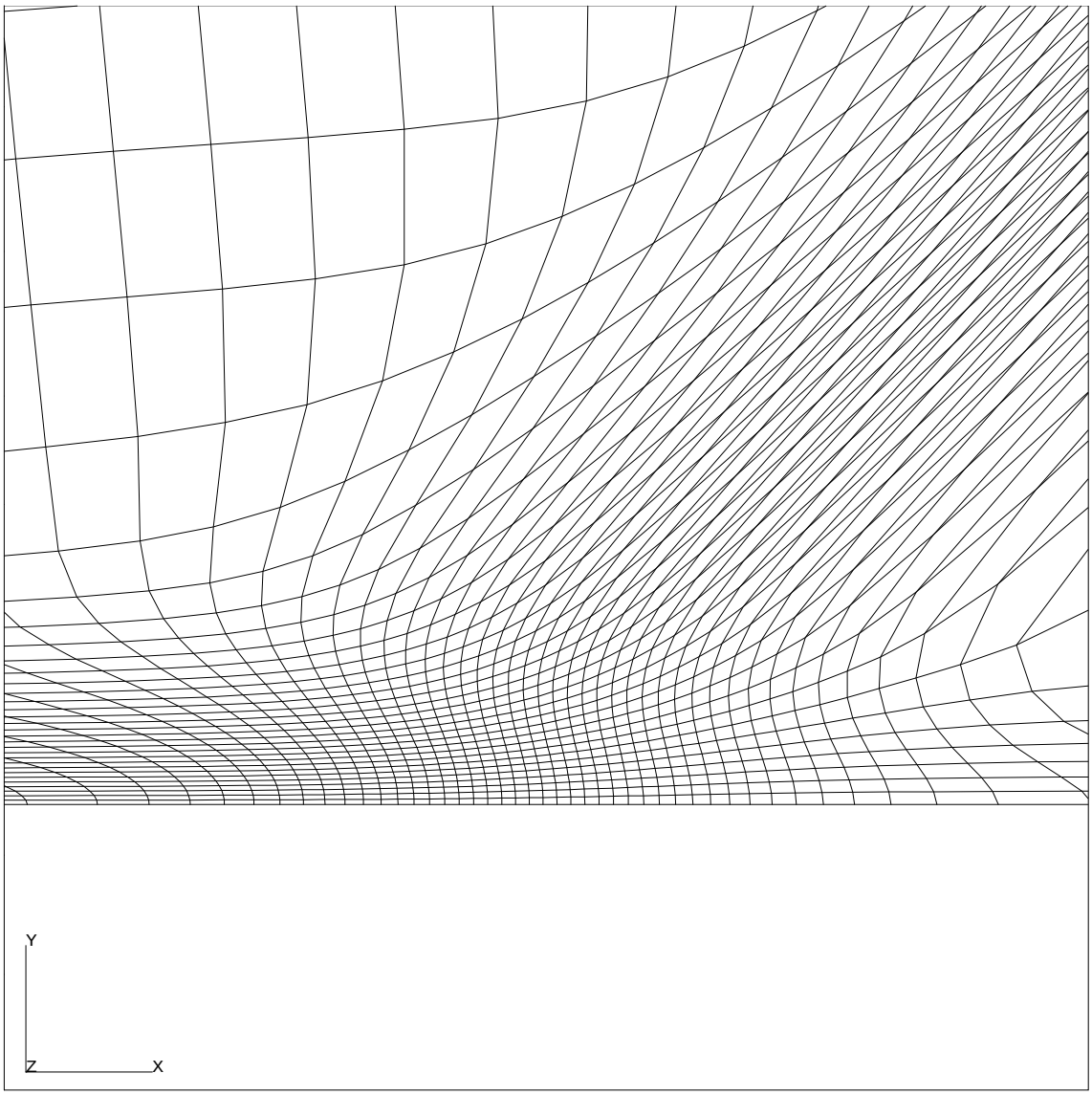


*Fig. 24 Detail of adapted grid at the foot of the shock.*

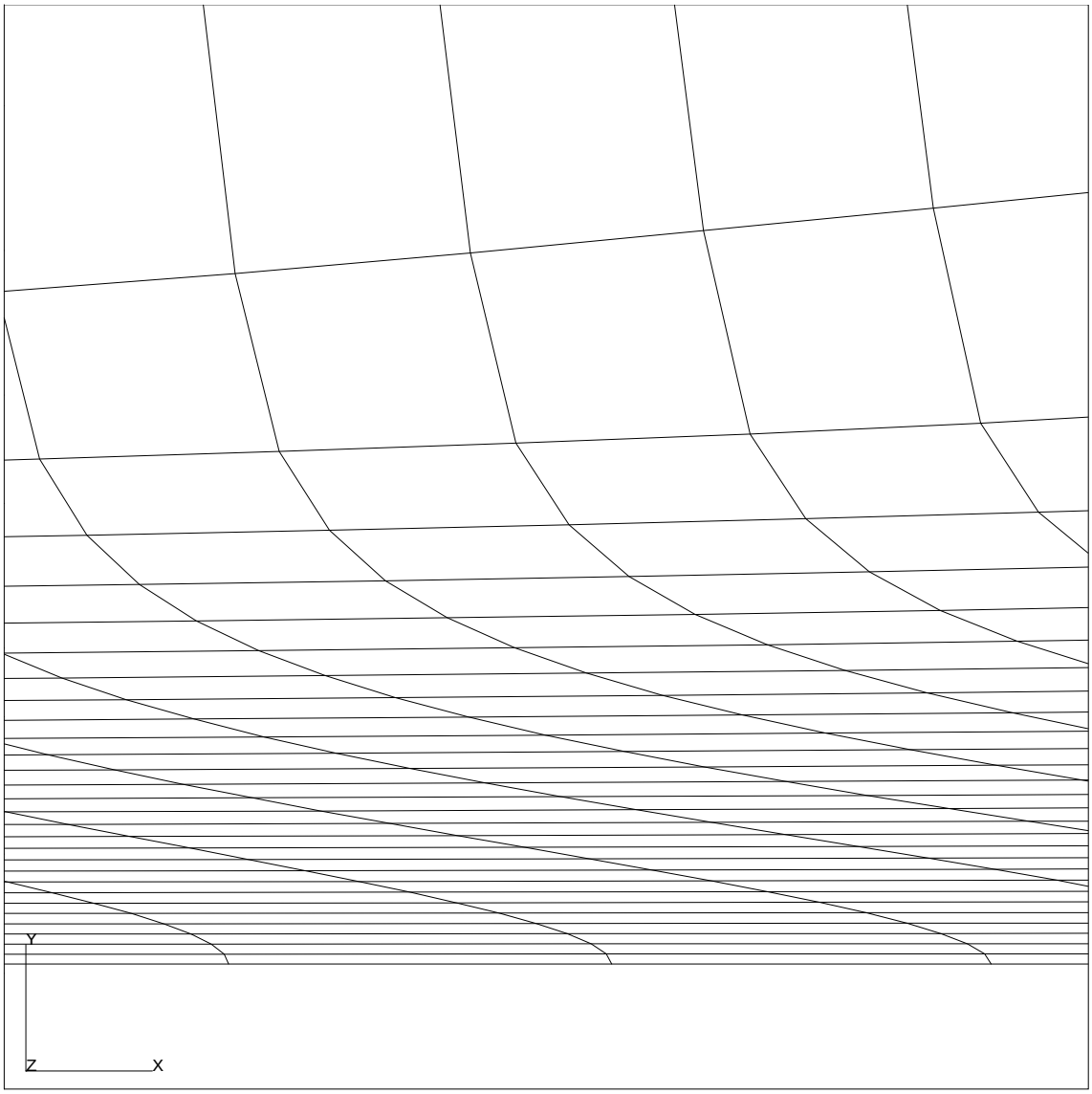


*Fig. 25 Detail of adapted grid in boundary-layer.*

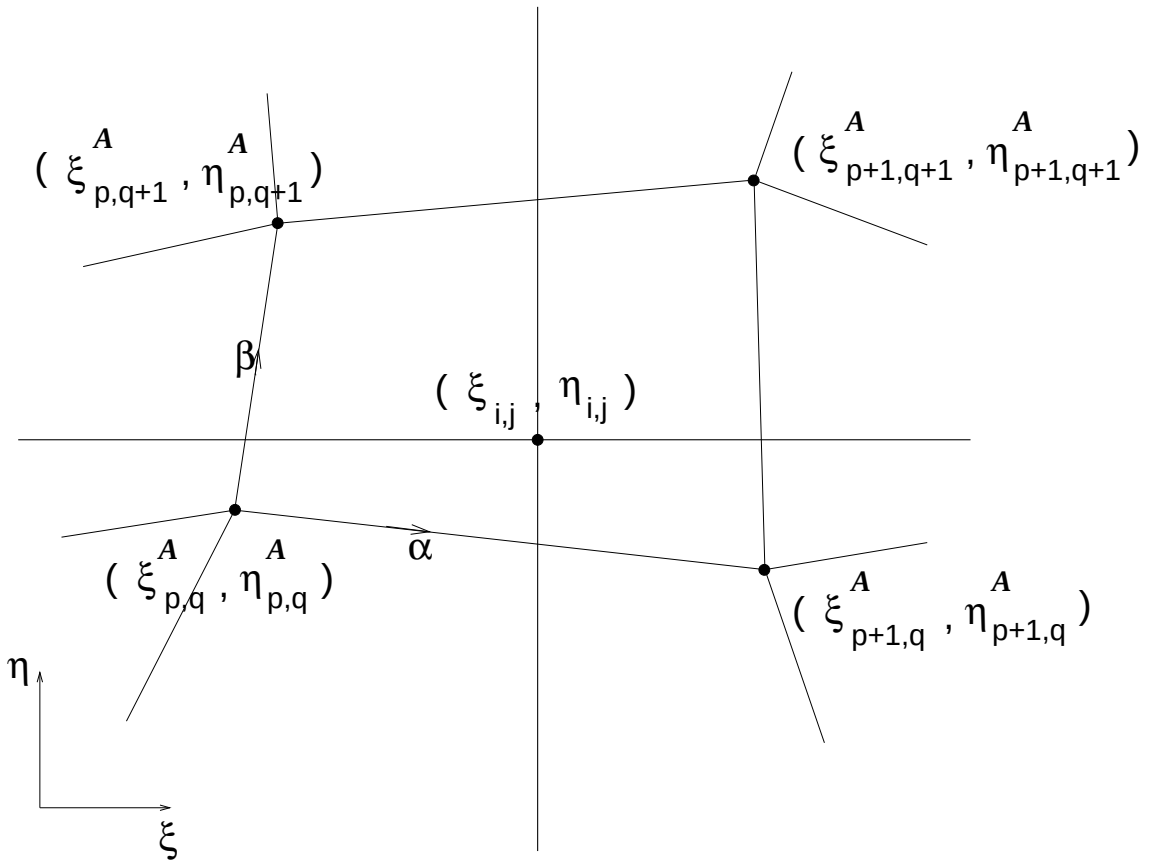


*Fig. 26 Patch (p,q) in parameter space $\mathcal{P}_{\xi\eta}$.*